12-15-2017

Enhancing iCVD Modification of Electrospun Membranes for Membrane Distillation through a 3D Printed Scaffold

Nicole Beauregard
nicole.beauregard@uconn.edu

Enhancing iCVD Modification of Electrospun Membranes for Membrane Distillation through a 3D Printed Scaffold

Nicole Beauregard

B.S., University of Connecticut, 2015

A Thesis

Submitted in Partial Fulfillment of the

Requirements for the Degree of

Master of Science

At the

University of Connecticut

2017

APPROVAL PAGE

Masters of Science Thesis

Enhancing iCVD Modification of Electrospun Membranes for Membrane Distillation through a 3D Printed Scaffold

Presented by

Nicole Beauregard, B.S.

Major Advisor_____
Daniel D. Burkey

Associate Advisor_____
Jeffrey R. McCutcheon

Associate Advisor_____
Aravind Suresh

University of Connecticut

2017

Acknowledgements

I would like to thank numerous people for their help and support on my master's thesis research project. First, I would like to thank my two advisors, Dr. Daniel Burkey and Dr. McCutcheon, for all their support and guidance on this project. I was able to learn and gain perspective on a wide variety of research areas. I would also like to thank my other committee member, Dr. Aravind Suresh, for beginning this research project and helping me gain confidence as a researcher.

I would also like to thank all of my current and former lab members. Thank you to Mustafa al-Furaiji and Matt Worthington for initially showing me how to use the equipment in lab. I would also like to thank Garrett Dias for all his help with the initial design and printing of the scaffold and Emily Fisler for all her help with the 3D printing. Thanks to Maqsud Chowdhury, Lingling Xia, Jian Ren, Basma Waisi, Wenming Hao, and Cong Ma for all the support and help in the lab. I would also like to thank Leah and Susan for all of their assistance and support as well.

Finally, I would like to thank my family and my friends for all their encouragement over the last two years. I would like to thank my parents, my sister, and my grandparents for believing in me and supporting me throughout grad school.

Table of Contents

i. List of Figures

ii. Abstract

In this work, initiated chemical vapor deposition, iCVD, is used as a modification technique for electrospun membranes. Electrospun membranes are often hydrophilic and cannot be used in membrane distillation which requires high hydrophobicity. In membrane distillation, a thermal driving force is supplied to create a vapor pressure difference across a membrane allowing vapor molecules to pass through while rejecting liquid and solids. iCVD can be used to conformally coat the individual nanofibers with a hydrophobic polymer to render the membrane viable for the MD process. The standard coating procedure uses natural convective diffusion as the method of transport of the hydrophobic coating monomer to the membrane. This procedure requires two sides of coating to achieve adequate hydrophobicity. We have altered this process by implementing a 3D printed scaffold to change the coating orientation of the membrane to force convective flow through the membrane effectively coating the membrane faster than traditional natural convective diffusion. It was found that this process reduced the coating time to 20 minutes compared to 200 minutes previously required for this membrane. It also eliminated the need to coat both sides of the membrane further reducing the process dead time. The membranes, themselves, also exhibited 100% salt rejection and a competitive flux value.

1. Introduction

1.1. Water Scarcity

Access to clean water is a fundamental human right essential to the fulfillment of life as decreed by The United Nations; yet, over 633 million people lack clean water [1,2]. The lack of clean water already accounts for over 800,000 childhood deaths each year and the ability to have clean water and sanitation has the potential to prevent about 6.3% of all deaths [3,4]. This problem is observed all across the world as shown in **Figure 1**. Water scarcity, where the demand for water exceeds available resources, can be divided into two categories: economic and physical water scarcity. In order to best mitigate the water crisis, it is important to understand the underlying causes of both economic and physical water scarcity.

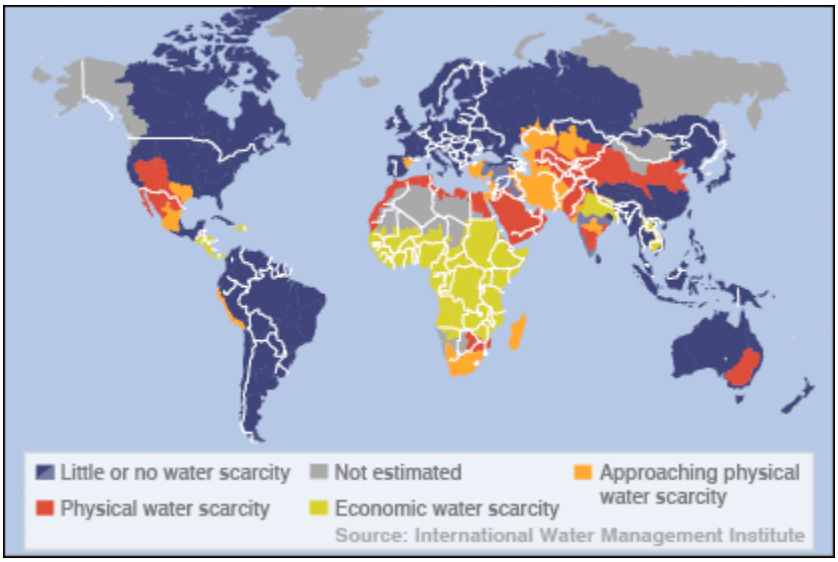

Figure 1: Map showing areas of physical and economic water scarcity across the globe [5]

Economic water scarcity occurs when there is a lack of water infrastructure to supply clean water due to a lack of available funding. While there is potential for an adequate supply of water to meet the demand, these areas do not have money available to obtain clean water. This

results in the use of unsanitary water from lakes and rivers, which can result in illnesses and deaths that are easily preventable. This form of water scarcity is prevalent in sub-Saharan Africa and Central America. Other parts of the world face a different form of water shortage. Physical water scarcity occurs when there is simply not enough water to satisfy the demand. This can be due to the increasing global population requiring more water for both domestic and agricultural resources, the overuse of the current renewable and nonrenewable resources, and the lack of precipitation, and droughts in arid regions that are increasing due to global warming [6]. Water scarcity is an issue all across the globe and is even becoming more prevalent in the United States.

California has recently experienced a physical water scarcity in the form of a record-breaking drought [8]. This caused the state to have to start using nonrenewable water resources in order to satisfy the demand. Fresh water accounts for only 2.5% of the water on earth. The majority of this water is predominantly inaccessible and trapped in the ground or as ice. Surface water, which is used to sustain daily life, accounts for only 1.2% of the fresh water supply [7]. This example of the overuse of surface water and the use of the nonrenewable resources reflects the further increase of water stress around the globe. While California is no longer in a state of drought, this still has a lasting impact on the water supply in California. In order to help mitigate water scarcity and create a more dependable water supply, drought resistant water sources are being explored to prevent future water shortages.

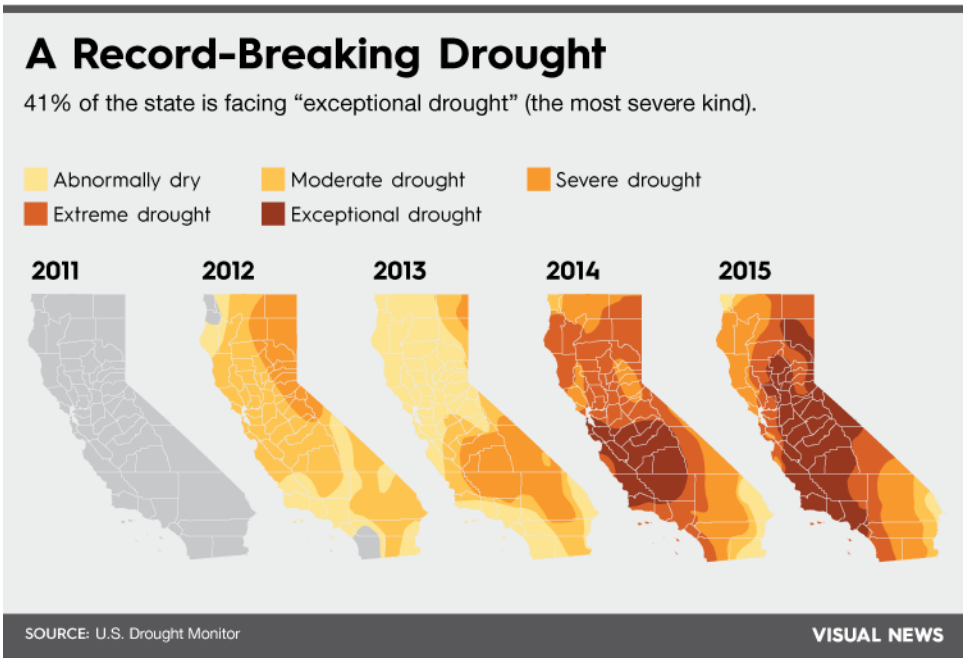

Figure 2: Regions of California experiencing drought conditions from 2011-2015 [8]

1.2. Desalination

One potential option for alleviating part of the water demand is desalination. The vast majority of the world’s water is saline and unsuitable for agricultural or domestic use. Desalination is the logical solution to solve the world’s water crisis; however, there are several drawbacks. While these processes can successfully produce clean water, they are also expensive to construct and operate. Desalination often produces a highly concentrated saline solution or brine. This brine needs to be disposed of safely and often needs to be diluted using additional water before it can be discarded. As the need for clean water continues to rise, the appeal of desalination increases even with the expense.

Desalination processes vary and are often driven by pressure, electrical, or thermal gradients. Reverse osmosis is a pressure-driven process where an external pressure is applied to a saline solution to overcome its osmotic pressure forcing water through a semipermeable membrane yielding pure water and a concentrated brine. The external hydraulic pressure is

required to overcome the natural osmosis process of water flowing from an area of high concentration to an area of low concentration. This process is the most extensively studied desalination technique and has been successfully implemented commercially. California has recently opened the Carlsbad desalination plant which uses reverse osmosis as the desalination tool to help alleviate some of the water scarcity in that region. Reverse osmosis has been well studied in literature and high-performance membranes and modules have been developed. While the high pure water yield and lower overall cost makes this more commercially desirable compared to other desalination methods, there are some drawbacks. Sufficient energy must be applied in order to overcome the osmotic pressure of the salt solution. As the salinity increases, this barrier becomes larger requiring more energy. There is a limit to how highly concentrated the feed solution can be, before reverse osmosis can no longer be used. Extensive and expensive pretreatment is required to eliminate contaminants and lower the salinity of the solution to prepare it for the reverse osmosis module.

One form of electrically driven desalination is electrodialysis. An electrochemical potential, acting as the driving force, is supplied across a semipermeable membrane to separate ions from a solution [9]. Unlike reverse osmosis, the ions, not water, pass through the membrane, which can increase the desalination rate. This process also benefits from low energy usage. Electrodialysis encounters problems when attempting to separate non-ionic components that are not affected by the electrochemical potential. Other desalination processes use thermal energy as a driving force. Conventional distillation is one such method. Unlike the previous methods discussed, conventional distillation is not a membrane-based approach. A series of heat exchangers or stages can be used to evaporate and condense steam from a contaminated feed to produce fresh water [10]. This distillation process is far simpler than the membrane-based

approaches and does not require the same level of pretreatment. This process is also able to achieve higher salt rejection than reverse osmosis. Distillation processes, however, require a large amount of energy to heat the solution to its high operating temperatures. There are also high maintenance costs associated with the equipment. An ideal desalination process would require low energy and no pretreatment, while producing clean water with high salt rejection.

2. Membrane Distillation

2.1. Introduction

Membrane Distillation (MD) is a thermally-driven desalination process that relies on a vapor pressure gradient to allow water vapor molecules to travel through a porous hydrophobic membrane while rejecting the salt and other contaminants contained in the liquid phase [11]. Several configurations of membrane distillation have been studied including direct contact membrane distillation, air-gap membrane distillation, vacuum membrane distillation, and sweep gas membrane distillation.

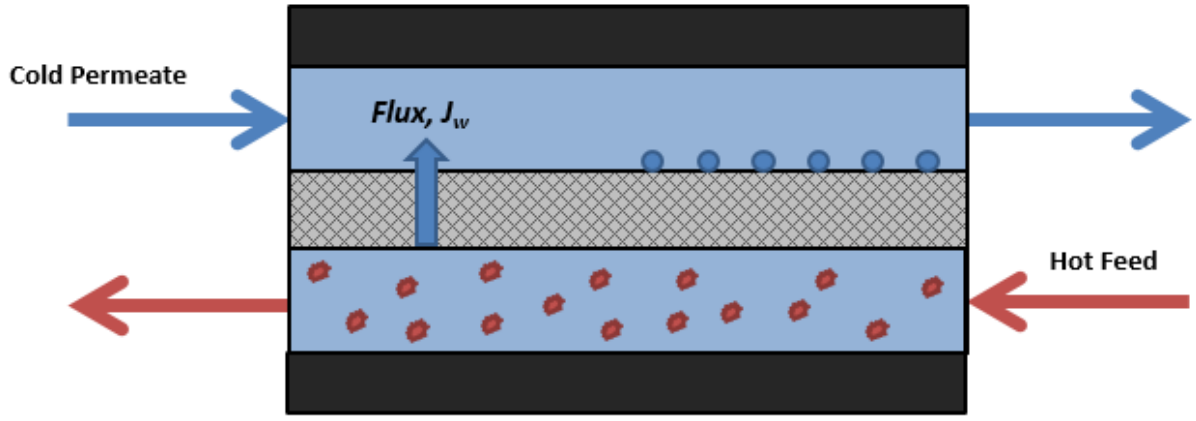

Figure 3: Direct contact membrane distillation (DCMD) schematic

Direct contact membrane distillation (DCMD) is the configuration investigated in this study. DCMD is the most extensively studied configuration and the simplest to set up on a benchtop scale. On one side of a semipermeable membrane is a hot feed stream. The other side contains a cold pure water stream generating the temperature gradient across the membrane. A water flux is observed as water vapor is permitted to travel from the hot feed stream through the membrane to the permeate side where it is condensed. While this configuration yields the highest water flux, it is subject to the highest conduction losses as both sides are in direct contact with liquid streams. The simplicity of the design allows this configuration to be the best option for this MD study.

2.2. Advantages and Disadvantages

Membrane Distillation, in general, is the intersection between traditional distillation and a membrane-based approach like reverse osmosis. The MD process uses a thermal gradient as the driving force for desalination, but can operate at lower temperatures due to the high membrane area-to-volume ratio [12]. Low grade heat can be used to achieve the necessary solution temperatures, alleviating some of the energy cost. Since the process relies on a thermal gradient rather than concentration gradient, MD does not encounter the same osmotic pressure limitation that reverse osmosis does. For high-salinity feeds where reverse osmosis fails, membrane distillation can be used instead. MD is also emerging as a desirable option in hybrid systems, coupling it with another process such as reverse osmosis for use in pretreatment applications.

MD membranes are prone to fouling due to their hydrophobic nature, which results in a loss of performance and wetting of the membrane over time. There is also heat loss due to conduction and mass transfer resistance through the membrane. One of the major drawbacks to the use of membrane distillation is the lack of suitable membranes available. This process has not

been as extensively studied as reverse osmosis and commercially viable membranes have not yet been produced.

2.3. Theory

In this process, there is both a mass flux of water vapor through the membrane, as well as a heat flux caused by the temperature differential between the two streams. Membrane design focuses on maximizing the mass flux, while minimizing the heat flux. In order to maximize vapor transport, it is beneficial to have a thin membrane, lowering the distance travelled for the vapor as well as low tortuosity and large porosity allowing for easier diffusion through the membrane. In heat transfer, it is most important to minimize conduction though the membrane by electing to fabricate membranes out of materials with low thermal conductivity. This minimizes the temperature polarization effect. The temperature polarization effect describes the reduction in thermal driving force due to boundary layer heat transfer resistances [13,14]. The thermal gradient that is created between the bulk fluid and the fluid bound to the membrane on both the feed and permeate side reduces the temperature difference across the membrane resulting in a loss of flux. The temperature polarization coefficient, shown in **Equation 1**, reflects how severe this effect is on the driving force and the overall flux. The temperature difference between the feed and permeate fluid bound to the membrane (T_{fm} - T_{pm}) is less than that of the bulk feed and permeate fluid (T_f - T_p). The actual driving force is lower due to the heat loss from the boundary layer effect.

$$\theta = \frac{T_{fm} - T_{pm}}{T_f - T_p} \quad (1)$$

A thicker membrane with low thermal conductivity will allow for better insulation lessening the temperature polarization effect. High porosity is beneficial to both mass and heat

transfer. Higher porosity yields more pores which allows for increased vapor transport through the membrane. The additional gas in the pores has a lower thermal conductivity than the membrane material lowering the overall thermal conductivity of the membrane.

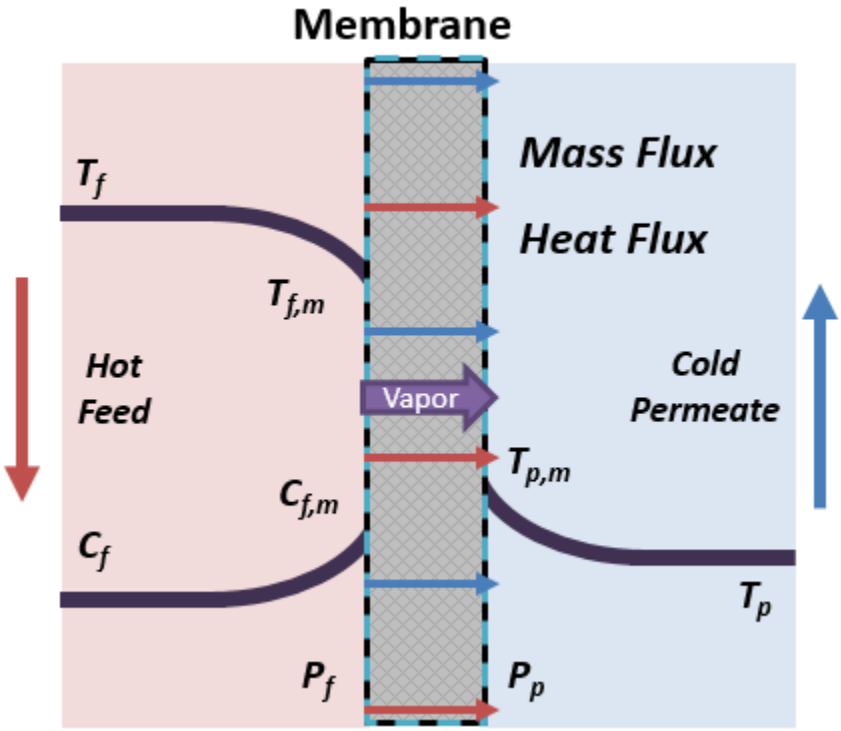

Figure 4: The mass and heat flux in direct contact membrane distillation (DCMD)

To maximize salt rejection, it is beneficial to have a membrane with a high liquid-entry pressure to prevent the membrane from wetting out and allowing liquid and contaminants to penetrate into the membrane. The minimum pressure at which the feed liquid will penetrate into the hydrophobic membrane pores and thus wetting the membrane is defined as the liquid entry pressure [15]. The liquid entry pressure is dependent on the hydrophobicity of the membrane defined as its contact angle (θ), the liquid surface tension (γ_L), and the maximum radius (r) and geometry (B) of the pores as shown in **Equation 2**.

$$LEP = \frac{-2B\gamma_1 \cos\theta}{r_{max}} \quad (2)$$

Liquid entry pressure increases with higher hydrophobicity. It also decreases with larger pore size. While smaller pore sizes are beneficial for salt rejection, larger pores are more beneficial for increased water flux creating an opportunity for design optimization. It is also important for a membrane to be robust and have high mechanical and thermal stability to withstand the process. Difficulty arises in finding materials and fabrication methods to produce high-performance MD membranes.

2.4. Common Materials Used

There are several membrane materials that have been used to produce viable MD membranes that are highly hydrophobic and also thermally stable. Common materials include Polytetrafluoroethylene **(**PTFE), Polypropylene (PP), and Polyvinylidene fluoride (PVDF). PTFE is a highly hydrophobic polymer and has shown good salt rejection and water flux in MD [16]. These membranes are manufactured through sintering and melt extrusion processes [17,18]. The main drawback to this material is its high cost, making it less commercially favorable. Polypropylene offers a low-cost alternative, but is only moderately thermally stable [19]. PVDF is less hydrophobic than PTFE, but also less expensive. PVDF also offers a unique property compared to other hydrophobic polymers in that it can be dissolved in solvents. This allows it to be used in a wider variety of polymer processing techniques rather than traditional sintering, melt-extrusion, or phase inversion processes. New polymer processing techniques can offer more of the desired MD properties than the traditional fabrication methods.

3. Electrospinning

3.1. Introduction

One method for manufacturing membranes that has shown good promise for use in MD is electrospinning [20]. Electrospinning is a polymer processing technique where a polymer is

extruded through a needle which is supplied with a voltage. The resulting fiber is collected in a random fashion on a grounded rotating drum. This creates a nonwoven mat suitable for membrane applications.

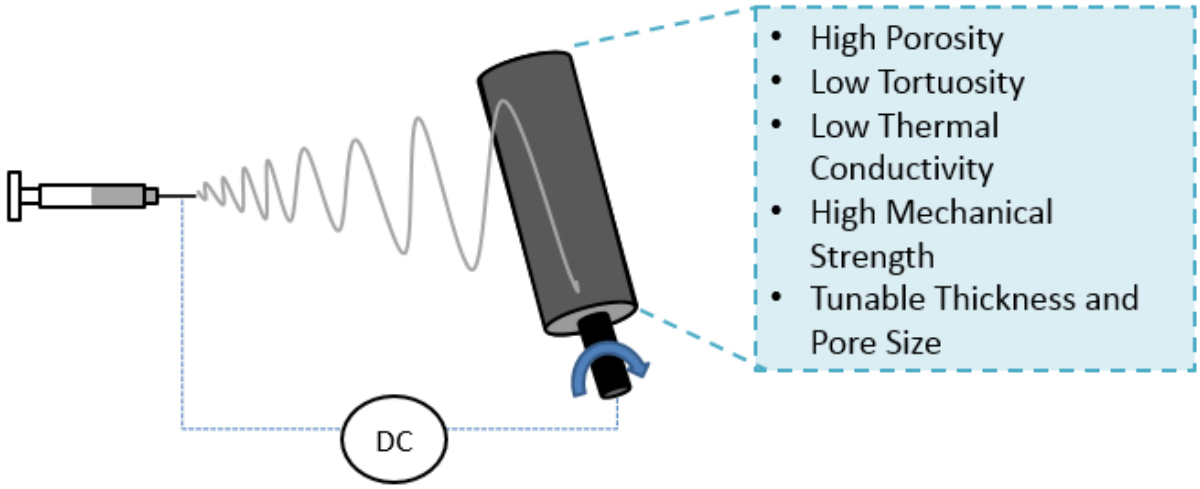

Figure 5: Electrospinning diagram and characteristics of electrospun membranes

3.2. Advantages and Disadvantages

These membranes offer many of the desirable characteristics of MD membranes including high porosity and a high strength-to-weight ratio [21]. The high porosity lowers the thermal conductivity of the membranes by the higher percentage of air trapped in the membrane, and also improves the water flux. The thickness of the membrane as well as the pore size can be tuned by changing the solution and spinning parameters, allowing for optimization of the membrane. This ability is instrumental in balancing the mass transfer and heat transfer effects in membrane distillation.

Spinnable hydrophobic polymers include PVDF, polystyrene, and polyimide [22–24]. Electrospun PVDF membranes have already shown good promise for use in MD [23,25]. PVDF was shown to exhibit a higher water flux than commercial, non-electrospun, PVDF membranes

[26]. This fabrication process for use in MD membranes is limited by the low availability of easily spinnable hydrophobic polymers. Electrospinning favors hydrophilic polymers which can be more easily dissolved in solution. A modification technique is required to render hydrophilic membranes hydrophobic in order to expand the range of polymers than can be suitable for use in membrane distillation.

The modification technique used cannot allow for any defects in the coating as this can allow for liquid passage through the membrane if there are any exposed hydrophilic areas. The membrane morphology should also be retained in order to maintain the desirable properties of electrospun membranes and to still allow for a high water flux. Modifying membranes to increase their hydrophobicity often results in a decrease in flux [27–29]. The addition of a coating decreases the pore size and also has the ability to completely clog pores. A coating technique that can provide a thin, uniform, and defect-free coating that maintains the membrane morphology is needed to render hydrophilic membranes suitable for MD.

4. Chemical Vapor Deposition

4.1. Introduction

Chemical Vapor Deposition (CVD) can be used to manufacture thin, uniform, and conformal coatings. CVD has been found to be a valuable method for polymer processing. These thin polymer coatings offer desirable properties including wear resistance, corrosion resistance, hydrophobicity, and lubricity. **Figure 6** shows the main intersection between CVD and polymers. Two forms of CVD, initiated chemical vapor deposition (iCVD) and oxidative chemical vapor deposition (oCVD), are especially valuable for polymer applications. CVD offers an innovative method for manufacturing thin polymer films which yield many unique properties unseen in other standard processing techniques.

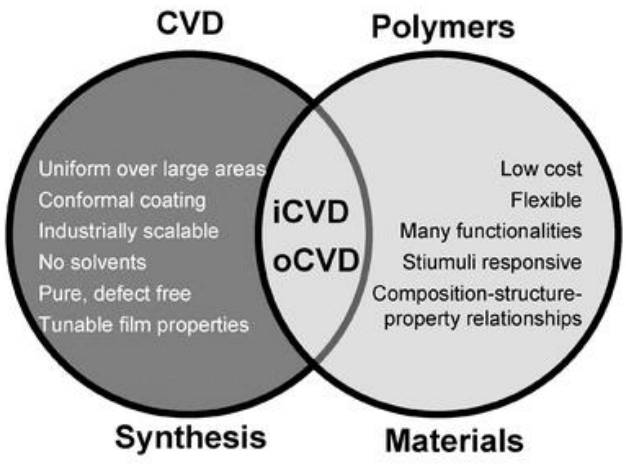

Figure 6: Relationship between chemical vapor deposition and polymers [30]

The CVD method is different than most coating techniques. The deposition process is conducted entirely in the vapor phase and does not require the use of a solvent [31]. Gaseous precursors are flown directly into the deposition chamber. Reactions occur in the gas phase and continue as the precursors adsorb directly onto the substrate allowing polymerization to then occur on the surface [32]. The gaseous precursors are converted directly to solid macromolecules creating a thin film with the complete exclusion of liquids. In most CVD applications, the rate limiting step is the adsorption of the monomer on the surface of the substrate [31]. Temperature, pressure, and concentration dictate the kinetics, and equilibria of the reactions [31]. The monomer saturation ratio shown in **Equation 3** is an important parameter for controlling and understanding the polymerization. P_m is the partial pressure of the monomer and P_{sat} is the saturation pressure of the monomer at the desired temperature [31].

$$S = {}^{P_m}/_{P_{sat}} \quad (3)$$

This ratio dictates many factors of the deposition including: the monomer concentration adsorbed on the surface, the growth rate, and the degree of conformality of the coating [31]. If

this ratio equals one, condensation will occur which obstructs the uniformity of the coating. The deposition chamber will also require an extensive cleaning procedure to remove the residual liquid. The ratio must be lower than one to avoid condensation; however, lowering the ratio yields less deposition.

The initiation process to begin the reaction differentiates the many types of CVD. Several types of chemical vapor deposition exist. Some of the more prominent polymer processing methods are initiated chemical vapor deposition, plasma enhanced chemical vapor deposition, and oxidative chemical vapor deposition. In the iCVD initiation process, a volatile initiator is flown into the reaction chamber and decomposes into free radicals when in contact with heated filaments inducing the free radical polymerization reaction. Each of these methods and their derivatives can be used to produce polymer films that can be used in many industrial applications.

4.2. Advantages and Disadvantages

There are many advantages for using CVD compared to other polymer processing techniques. CVD can be used to fabricate high-quality thin films. These thin polymer films deposited using CVD are conformal and are of uniform thickness and coat evenly over every contour of a geometric shape [31]. This is more difficult to achieve in liquid based coating techniques. In the liquid phase, surface tension affects conformality as the liquid molecules adhere to each other. This makes it challenging for the solution to penetrate into small cavities. It is also possible for the solution to collect in larger cavities, resulting in an uneven coating. In comparison, the vapor phase monomers do not exhibit this cohesive property which facilitates the penetration of vapor molecules into small cavities and can more evenly coat larger pores. Conformality preserves the geometry of the substrate after coating, which can be crucial for

many industrial applications. The coatings are also durable which is due to the crosslinking of the coated polymers and covalent bonding at the interphase between the polymer and substrate [31]. Certain chemical agents can be added to the polymer solution to promote crosslinking. Most precursors for CVD are commercially available and do not require further synthesis which makes the process more adaptable for scale up and industrial purposes [33]. The thin films produced by CVD are uniform, conformal, and durable which can be difficult to achieve in other processes.

CVD can produce polymer films of higher purity than other methods. The liquid monomer must be in the vapor phase before it can enter the reaction chamber, so low molecular weight monomers are preferred as they are more easily volatilized. These monomers can be purified to a higher degree than heavier ones [31]. CVD also yields purer polymer films compared to liquid-based deposition methods. Residual solvents can introduce impurities into the film. The solvent could also react with the polymer and cause chemical or physical changes to the film. Since any potential solution effects are avoided, the properties of the polymer can more easily be retained using this technique. CVD is also beneficial for insoluble polymers, electrically conductive polymers, and other polymers that are not compatible with solvents widening the range of polymers that can be deposited [33]. CVD can be used as an innovative technique for processing polymers that are not compatible with solutions or lose chemical functionality in solution.

In addition to expanding the variety of polymers that can be fabricated, a vast array of substrates can also be coated using this process. Due to its solvent-less nature, CVD is ideal for deposition onto substrates that may swell, degrade, or react when in contact with solvents [31]. CVD also operates at a low surface temperature yielding less thermal stress, which enables

polymer deposition onto heat sensitive substrates. Similarly, a drying step is not necessary which could potentially damage substrates. There are also no curing or sintering steps required in this method. This gentle deposition method also has low process power, which ensures that fragile substrates will not be damaged or deformed after the process [33]. Highly porous and high-aspect-ratio substrates, such as membranes, benefit from CVD due to the conformal nature of the coating and the gentle nature of the deposition process.

While this process is advantageous for many polymers, there are some disadvantages to CVD. One disadvantage is that there can be waste produced. There is low efficiency for the precursors used as not all the monomer and initiator are adsorbed onto surface [32]. This results in waste that must be safely disposed of. The monomers and initiators can be toxic or harmful to the environment. Adequate venting and disposal protocol are necessary as recycling the precursors is incredibly difficult. The reaction chamber also requires frequent cleaning as the polymer also deposits on the chamber walls and lid in addition to the substrate [32]. Certain monomers have long deposition times and the process is not continuous making it less commercially desirable to mass produce coatings. Even with the few disadvantages, the unique advantages CVD can bring to polymer processing are increasingly of interest for research and industrial applications.

4.3. Initiated Chemical Vapor Deposition (iCVD) Theory

There are several different types of chemical vapor deposition for producing thin polymer films. Initiated Chemical Vapor Deposition (iCVD) is the most extensive and most widely studied technique for polymer applications. The general mechanism of the process is free radical polymerization. **Figure 7** shows a simplified schematic of the process and a diagram of the deposition chamber. The substrate, or the supporting material for the polymer, is placed on the

stage inside the chamber. Stage temperature is controlled by an external chiller. The heated filament array is suspended above the stage and usually maintained around 200-400°C which is used to decompose the initiator. This creates a temperature gradient between the filament array and the stage. When the experiment is running, the chamber pressure is controlled via a vacuum pump and a constant pressure is maintained that corresponds to P_m or the partial pressure of the monomer. The optimal deposition conditions vary for the specific polymer used.

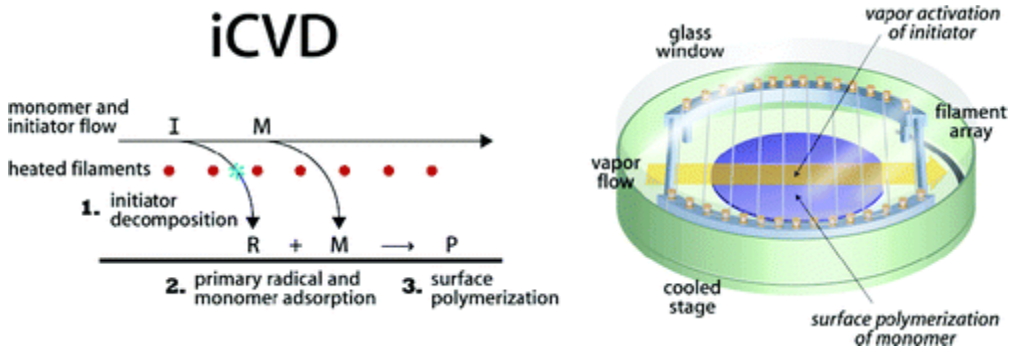

Figure 7: General overview for the iCVD process and deposition chamber diagram [34]

The individual reactions for the free radical polymerization are depicted in **Table 1**. First, the liquid monomer (M) and initiator (I) are volatilized and then flown into the reaction chamber. Heated filaments are then used to decompose the initiator into free radicals (R). The free radicals and monomers adsorb onto the surface through primary radical adsorption and monomer adsorption. Free radical polymerization then occurs on the surface of the substrate to produce the thin polymer film. The free radical polymerization consists of three steps: initiation, propagation, and termination.

Table 1: Free Radical Polymerization Mechanism for iCVD [35]

Gas Phase	Gas to Surface	Surface (Free Radical Polymerization)
Initiator Decomposition: $I(g) \xrightarrow{k_d} 2R \bullet (g)$	**Primary Radical Adsorption:** $R \bullet (g) \xrightarrow{k_{ad,R}} R \bullet (ad)$ **Monomer Adsorption:** $M(g) \xrightarrow{k_{ad,M}} M(ad)$	**Initiation:** $R \bullet (ad) + M(ad) \xrightarrow{k_i} M_1 \bullet (ad)$ **Propagation:** $M_n \bullet (ad) + M(ad) \xrightarrow{k_p} M_{n+1} \bullet (ad)$ **Termination:** $M_n \bullet (ad) + M_m(ad) \xrightarrow{k_t} M_{n+m}(ad)\ and\ M_n(ad) + M_m(ad)$ **Primary Radical Termination:** $M_n \bullet (ad) + R \bullet (ad) \xrightarrow{k_t'} M_n(ad)$ **Primary Radical Recombination:** $R \bullet (ad) + R \bullet (ad) \xrightarrow{k_t''} R_2(ad)$

Film thickness can be measured using laser interferometry. This value can be used to calculate the deposition rate shown in **Equation 4** [36]. The thickness, d, is multiplied by N, the number of 2π cycles observed in the sinusoidal interferometry plot produced and divided by the deposition time. The rate can also be related to activation energy (E_a) and temperature. The process is adsorption limited and the deposition rate increases with decreasing stage temperature [36]. The thickness can be easily monitored and controlled using this technology.

$$Rate = \frac{\Delta d_{film} * N}{\Delta t} = Ae^{-E_a/RT} \quad (4)$$

iCVD is especially useful for preserving the organic functionality of the monomer compared to other types of CVD. iCVD can produce linear polymer chains that retain their structure [37]. For example, the energetic plasma used in plasma enhanced CVD (PECVD) to initiate the reaction can damage the organic polymer [33]. The monomer is prone to fragmentation, which can destroy some of the important functional groups on the monomer. Since iCVD polymerization only uses minimal heat to decompose the initiator and no additional energy or stress, the functional groups are more easily retained as the monomers do not degrade under these conditions. Also, since the operating temperatures for iCVD are relatively low, it

requires less energy to run the process. The low temperature is favorable for deposition onto most substrates as well and for the preservation of substrates.

4.4. Applications for Membrane Modification

CVD offers the ability to produce thin, conformal, polymer coatings of high quality that can be utilized in a variety of important applications including membrane modification. CVD can be used to generate antifouling or antibacterial coatings, which is especially pertinent for MD membranes where fouling is a major problem. Since CVD is a gentle and conformal technique, substrates can be coated and still retain their morphology and properties. Individual fibers of porous materials can be coated and maintain their appearance and texture. One study proved the antimicrobial ability of CVD polymers by coating nylon cloth with poly(dimethylaminomethyl styrene) [38]. The coating was found to be effective at killing both Escherichia coli and Bacillus subtilis over one hour. CVD coatings can also be used as antifouling agents. Another study used iCVD to deposit a thin polymer film of poly[N,N-dimethyl-N-methacryloxyethyl-N-(3-sulfopropyl)-co-2-(dimethylamino)ethyl methacrylate-co-ethylene glycol dimethacrylate], or PDDE, which has zwitterionic functionality [39]. This process is gentle enough to be able to deposit onto membrane and maintain the functional amine groups of the polymer. The zwitterionic coating was shown to have low adsorption of many potential foulants including humic acid, sodium alginate, and bovine serum albumin. These films also are highly biocompatible.

Another application for CVD polymers, especially relevant to membrane distillation, is forming thin hydrophobic or nonstick coatings. Due to its conformality, CVD can coat the entire area of a substrate. This allows for minimal defects in the coatings and can therefore result in a hydrophilic substrate becoming completely hydrophobic after coating. As mentioned previously,

electrospun membranes have many of the desirable qualities for use as membrane distillation membranes. The one drawback is that most easily spinnable membranes are hydrophilic. In MD, hydrophobic membranes are required as aqueous solutions are in contact with the membrane. A hydrophilic membrane would wet out when in contact with the solution and allow the salt solution to travel through the membrane. One study used iCVD to deposit a hydrophobic polymer coating onto a hydrophilic membrane [40].

The authors coated a hydrophilic polyamide membrane with poly(1H,1H,2H,2H-perfluorodecyl acrylate) or PPFDA. The electronegative fluorine atoms create a hydrophobic polymer chain. The individual fibers comprising the electrospun membrane were coated with this polymer, highlighting the conformal nature of this process. The dramatic increase in contact angle reflects its new hydrophobicity as a result of the coating. This membrane also exhibited high water flux or water diffusion through the membrane and yielded high salt rejection values. This suggests the coating was uniform as salt was not allowed to pass freely through the membrane. CVD can offer a valuable technique for improving the hydrophobicity of membranes while maintaining the integrity of the membrane itself.

The CVD process has also been developed for commercial use. Thin polytetrafluoroethylene or PTFE coatings can be also produced using CVD. PTFE is known for its hydrophobic properties and its similarity to Teflon. GVD Corporation currently produces their own commercial PTFE coating which displays the same bulk properties as Teflon [41]. This product can be used as a water repellent for clothes and fibers, and as a nonstick coating. The coating has also found value in the automotive industry as a coating for tire molds [42]. The conformal, and solvent-free PTFE coatings produced through CVD have been shown to be a commercial success and pave the way for future companies to invest in this technology. In terms

of a modification technique for MD, there is the potential for this process to be scaled up for commercial production to produce hydrophobic membranes from hydrophilic substrates.

4.5. Typical Polymers

A wide array of polymers can be fabricated using CVD technology. For iCVD, it is important for a monomer to be easily volatilized from a room-temperature liquid state. iCVD favors low-molecular-weight monomers which can be more easily purified to produce higher-quality films. While the operating temperature is relatively low, the monomer must be able to withstand some radiation and heat transfer via convection from the heated filaments. Some commonly used monomers for this process include acrylates, methacrylates, vinyls, and styrenes. Fluorocarbons including PTFE and PVDF can also be deposited using this polymer processing technique [31]. CVD can also be used to form copolymers. Most volatile monomers can be manufactured using this process, which allows for more research into new polymers and new applications for these polymers including use as coatings for MD membranes.

4.6. Conclusion

Chemical Vapor Deposition is a promising technique for polymer processing that can be extended to membrane applications. Companies like GVD have been successful in manufacturing large-scale reactors to commercialize these products. CVD offers industry a solvent-free process, and can provide conformal, uniform, defect-free coatings of high quality. This makes iCVD the most suitable option for nanofiber membrane modification. As shown previously, this technique has been successful in fabricating suitable MD membranes from hydrophilic substrates, yet there are still many avenues that need to be explored to make this process more commercially viable.

5. Background and Objective

Membrane Distillation (MD) is a thermally-driven desalination process that relies on a vapor pressure gradient to allow vapor molecules to travel through a porous hydrophobic membrane while rejecting the salt [11]. One of the main limitations with this technique is the lack of suitable membranes. A MD membrane must first be hydrophobic and ideally exhibit many other properties including: high porosity, low tortuosity, low thermal conductivity, and high dimensional and thermal stability [43]. Electrospun membranes offer many of the desirable characteristics of MD membranes including high porosity and a high strength-to-weight ratio [43]. Also, many membrane properties including fiber diameter and thickness can be easily optimized by altering the solution and spinning parameters. Electrospun PVDF membranes have already shown good promise for use in MD [22,23,25]. This fabrication process, however, is limited by the low availability of easily spinnable hydrophobic polymers. Electrospinning favors hydrophilic polymers that can be more easily dissolved in solution. Therefore, a modification technique is required to render hydrophilic membranes hydrophobic and suitable for membrane distillation

Initiated Chemical Vapor Deposition (iCVD) has emerged as a viable modification technique for porous membranes [44–47]. The solvent-free nature of this process allows for a uniform, conformal coating allowing the morphology of the membrane to remain intact. This process facilitates the formation of pure, defect-free films compared to conventional solvent-based techniques. The use of solvents can add potential impurities into the coating, and solvents may also react with monomers forming undesirable side products. Monomers used for iCVD must be easily volatilized. This favors low molecular weight monomers which are easier to

purify. iCVD is also suitable for fragile or heat-sensitive membranes as the substrate is not directly exposed to high temperatures or any stress during the process.

iCVD has been used to increase the hydrophobicity of hydrophilic substrates [48,49]. A hydrophobic polymer can be uniformly and conformally deposited on the substrate altering its surface properties. One hydrophobic polymer, PPFDA, has successfully been used to render hydrophilic electrospun membranes suitable for MD, however, this polymer can no longer be used commercially due to environmental concerns [40]. Divinylbenzene (DVB) has emerged as a more environmentally friendly alternative, but the deposition time required to achieve suitable hydrophobicity is much longer [50].

This objective of this work is to enhance the iCVD coating process of porous membranes via the addition of a 3D printed scaffold. The scaffold will be span the height and width of the chamber and suspend the membrane in a new orientation normal to the flow of reactants into the chamber. In the standard process, the membrane is affixed to the cooled stage at the bottom of the chamber. Deposition occurs as the reactants diffuse to the bottom of the chamber and adhere onto the fibers. The majority of the reactants do not polymerize and are expelled out of the chamber through a vacuum pump. The scaffold, on the other hand, will harness the effect of convective flow of the reactants through the membrane as they are pulled towards the vacuum on the other side of the scaffold. The only path for the reactants to the vacuum is through the porous membrane, which would allow for a higher conversion of monomers, limiting the potential waste. One other drawback with the standard procedure is that the membrane must be coated on both sides in order achieve adequate hydrophobicity. Once one side has been coated, the chamber must be purged and opened to flip the membrane over. By suspending the membrane in the scaffold, the convective flow of the reactants can allow for adequate coating on both sides of

the membrane, eliminating the dead time required to flip sides. This work aims to investigate a new method for coating porous media to make the process more efficient, reducing both time and waste.

6. Materials and Methods

6.1. Materials

Polyacrylonitrile (PAN, MW=150,000) was purchased from Scientific Polymer Products (Ontario, NY). N, N-dimethylformamide (DMF, anhydrous, 99.8%) was purchased from Acros Organics. Sodium chloride (NaCl, crystalline, certified ACS) was obtained from Fisher Scientific (Pittsburgh, PA). Divinylbenzene (DVB, Sigma Aldrich, Technical Grade, 80%) and *tert* butyl peroxide (TBPO, Sigma Aldrich, 98%) were used as purchased with no further purification.

6.2. Electrospinning Protocol

PAN and PVDF nanofiber mats were produced in a custom-built electrospinning chamber. To prepare the 8% PAN solution, PAN polymer powder was dissolved in DMF and stirred for 24 hours at 60°C. 20 mL of polymer solution was spun and collected on a rotating drum covered with aluminum foil at a rate of 1.5 mL/h. The voltage was maintained between 22-28 kV and the relative humidity in the chamber was maintained at around 20%. To prepare the 8% PVDF solution, PVDF polymer powder was dissolved in a 60:40 ratio of DMF and acetone. The solution was stirred for 24 hours at 60°C. 20 mL of solution was electrospun onto a fabric sheet at a rate of 4 mL/h. The voltage was between 22-28 kV and the relative humidity was maintained at 40%.

6.3. Scaffold Manufacture

A schematic of the 3D printed scaffold was first designed using SOLIDWORKS computer aided design software. Before beginning, several design criteria were set forth. The device should be able to support an electrospun membrane vertically for the duration of the experiment and allow for the reactants to flow through unobstructed. The scaffold should also conform to the chamber geometry in order to maximize flow through the membrane and prevent flow through gaps between the chamber and device. The filament array must be allowed to pass through the scaffold as it encompasses the whole chamber and cannot be rearranged. These criteria influenced the original design and design iterations of the scaffold.

Design 1 was the first iteration of the scaffold and was never 3D printed. It was determined that the air vents included in the design to prevent a potential pressure build-up of reactants were not necessary. The porous nature of the membrane would allow for adequate flow of the reactants through it and not result in any build-up. Also, the device did not conform to the geometry of the chamber. More accurate measurements needed to be included into this design. The exact geometry of the chamber was not taken into consideration and only rough estimates were made. The area in the center of the device where the membrane would be exposed to the reactants was also too small, and the membrane coated would not be suitable to be tested using the benchtop system. This iteration also did not allow enough room for the filament array to sit. With these points taken into consideration, Design 2 was constructed.

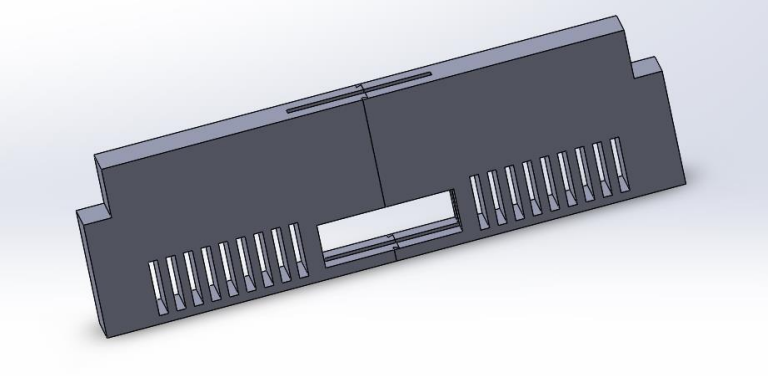

Figure 8: Scaffold Design Iteration 1

The geometry of the device was altered to better conform to the chamber. The changes included the small indentations on the bottom corners of the device and the increased indentations on the top two sides for the filament array to rest. Blocks were also created to sit on top of the array to further block flow. This design also featured the first iteration of the membrane stage. In order to support the membrane, a stage was designed for the membrane to sit. While the original idea was to slide the membrane inside the stage, it was determined that placing the membrane on top of a fine mesh would allow for better support. The stage would then be placed into a slot at the top of the scaffold where the membrane would rest in the open area of the scaffold.

This iteration was the first one to be 3D printed. Due to size limitations with the 3D printers used to fabricate this device, it was determined that the scaffold must be printed in two separate parts and then joined together. Joints were added to this design to be able to slide the two halves together to form one cohesive piece. The membrane stage design allowed for additional connection between the two sides to improve the stability of the device. The membrane stage has two wider areas at the top which fit into the respective cutouts on each of the two parts further securing the device together as shown in **Figure 9**. After printing, it was

found that the tolerances used to allow for the joining of the various pieces were not large enough. The two sides could not be joined together and the blocks were also not able to fit on the sides supporting the filament array as well. It quickly became evident that more iterations needed to be made to this design.

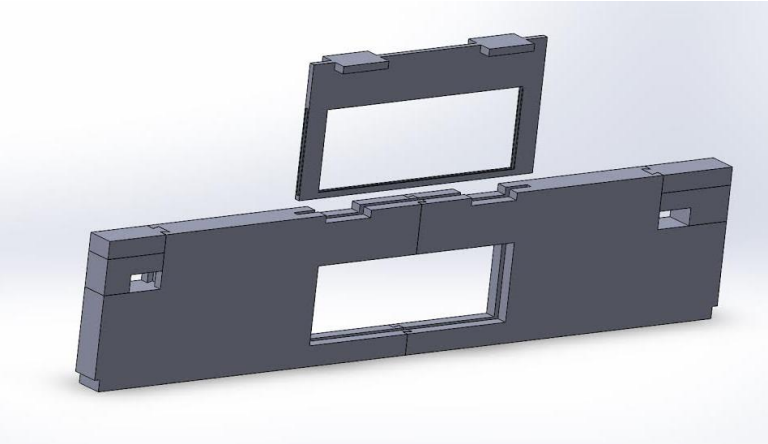

Figure 9: Scaffold Design Iteration 2 showing geometry modifications including the membrane stage and caps to enclose the filament array within the device

Design 3 was quite similar to the previous design. Larger tolerances were added to allow for the pieces to be easily connected. Unnecessary area was also removed to shorten printing time. When printed, it was found that the device fit perfectly into the chamber. The device, however, did not allow for the filament to sit in the chamber. The gap between the top indentations was too wide and the filament array sat too high in the chamber which would affect initiator decomposition. It was also observed that one side of the array required the filament to be strung which required more room on that side. There was also a concern of potential melting if the filament was in direct contact with the device. With the general geometry determined, the new iteration focused on redesigning the filament array section.

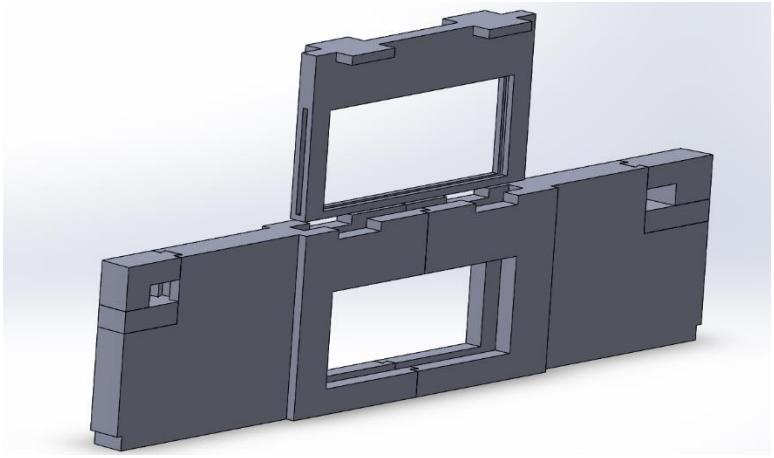

Figure 10: Scaffold Design Iteration 3 showing the geometry changes

Design 4 is the current iteration of the scaffold. The filament array section was completely redesigned. The gaps where the filament array sits have been extended so it can rest closer to the bottom of the chamber. Blocks have been designed to allow for the height to be adjustable to achieve the desired filament height. The blocks no longer used dovetail joints to connect to the chamber, but a tongue and groove joint, which requires lower tolerances and is more easily sanded. In order to support the membrane, a mesh was also 3D printed to rest within the stage. It was also discovered that the top of the device was not in direct contact with the lid. Clay was used to determine the exact gap and caps were designed. This allowed us to not have to reprint the entire device, while also covering the slight gap created at the top via the blocks. This completed design met all the design criteria required for experimentation.

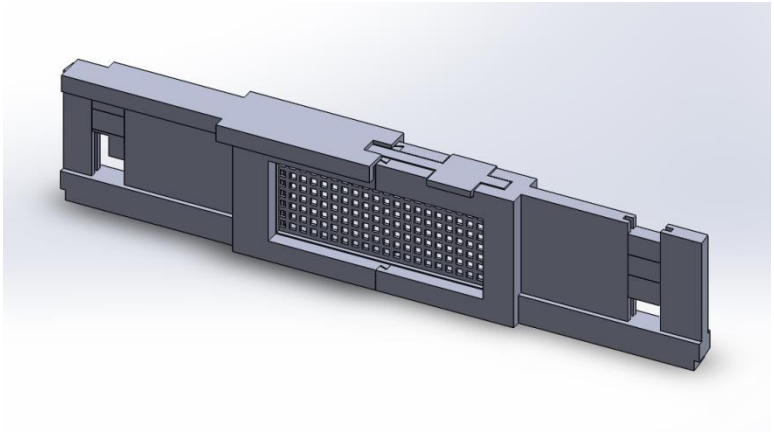

Figure 11: Final Scaffold Design showing the redesigned area to hold the filament array, the caps to achieve better contact with the top of the chamber, and the mesh to support the membrane in the device

The device was manufactured using a Formlabs Form 1+ 3D printer. This type of printer utilizes a form of 3D printing called stereolithography. In this process, a photo-reactive liquid resin is cured via a system of lasers and mirrors causing localized photopolymerization [51]. The tank containing the resin is stored at the bottom of the printer and the device is printed from the bottom upwards. As the each new layer is printed, the platform holding the device lifts the newly cured layer higher above the resin tank allowing the next layer to be cured. When the piece is fully printed, it is lifted entirely out of the tank. Residual resin is washed away from the device in a bath of isopropyl alcohol. The final piece can then be sanded to eliminate any imperfections created during the print.

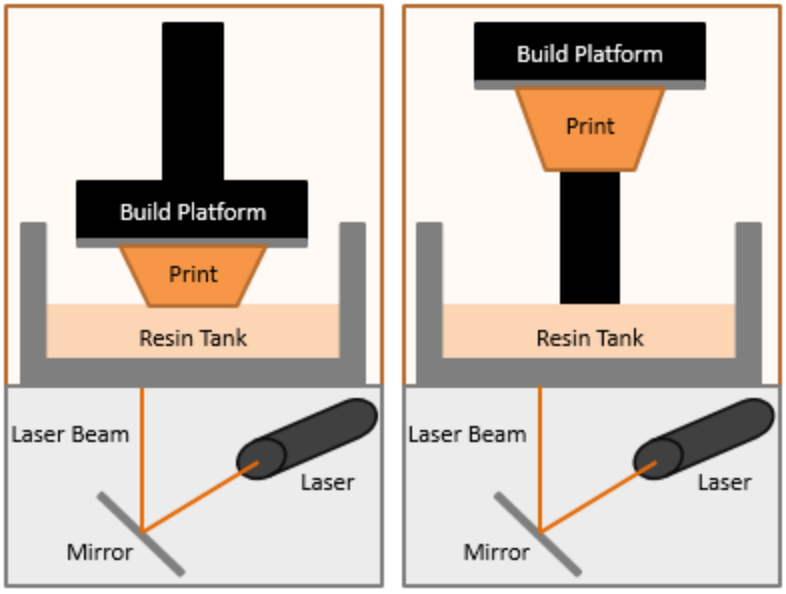

Figure 12: Stereolithography 3D Printing Schematic

While this form of 3D printing allows for better resolution, there were some problems encountered during the process. During printing, supports are created to adhere the piece to the platform and prevent the piece from warping. These supports can be removed using flush cutters after the residual resin is removed and the piece has been dried. While these supports are necessary, they can be difficult to remove completely and often leave imprints of where they were attached. It is a balance between potential warping and precision when determining where to place the supports. Several times during the printing process, the device failed to print or exhibited warping that inhibited it from being used.

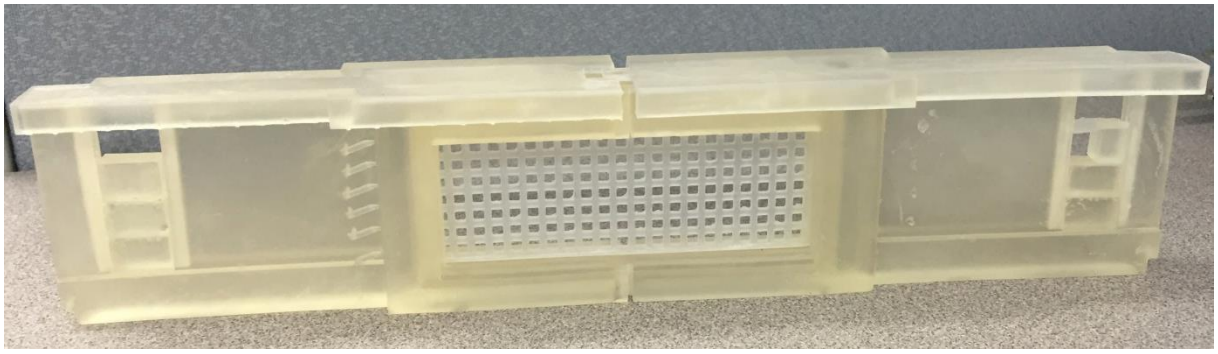

Figure 13: 3D Printed Scaffold

After several iterations, the 3D printed scaffold was successfully manufactured. Before experimentation, the device was tested for its heat resistance at 60°C and tolerance to the reactants used in the chamber. It exhibited no change after being exposed to either. The device was then deemed suitable for experimentation.

6.4. Initiated Chemical Vapor Deposition Protocol

iCVD experiments were conducted in a custom-built reactor (GVD Corporation). The initiator, tert butyl peroxide (TBPO), was flown into the chamber in the vapor phase at rate of 15.0 sccm using a mass flow controller (MKS 1479). TBPO was held at ambient temperature due to its high volatility. The monomer, divinylbenzene (DVB), was heated to 70°C and flown in the chamber at a rate of 3.0 sccm through a delivery line heated at 80°C to prevent condensation. To prevent auto-polymerization, copper chloride ($CuCl_2$) powder was added to the vessel containing liquid DVB. A vacuum pump (Edwards E2M40), pressure transducer (MKS 622), and throttle valve (MKS 153D) were used to maintain the pressure in the chamber at 150 mTorr. The temperature of the stage was controlled using a water-cooled chiller held at 12°C. Electrically heated nichrome filaments (Omega NI80-111 020) were suspended above the cooled stage and were maintained at 300°C.

The scaffold was set approximately in the center of the chamber effectively dividing the chamber into two halves. The filament array was only strung across the half of the chamber before the scaffold while the half facing the vacuum pump was empty. To ensure deposition was occurring, a silicon wafer was placed beneath the filaments and laser interferometry was used to measure the thickness of the polymer film. The membrane to be coated using the new approach was placed on the membrane stage of the 3D-printed scaffold and supported by a thin mesh. The membrane stage was then slid into place in the scaffold to suspend the membrane above the chamber stage and in normal flow to the reactants. A control membrane was also taped to the bottom of the stage below the filament array in accordance with the standard deposition method. Deposition of pDVB was first conducted over a range of times between 50-200 minutes. The membranes were not flipped during the process for either the standard method or the new approach. The data presented reflects only one side of the membrane being in direct contact with the reactants.

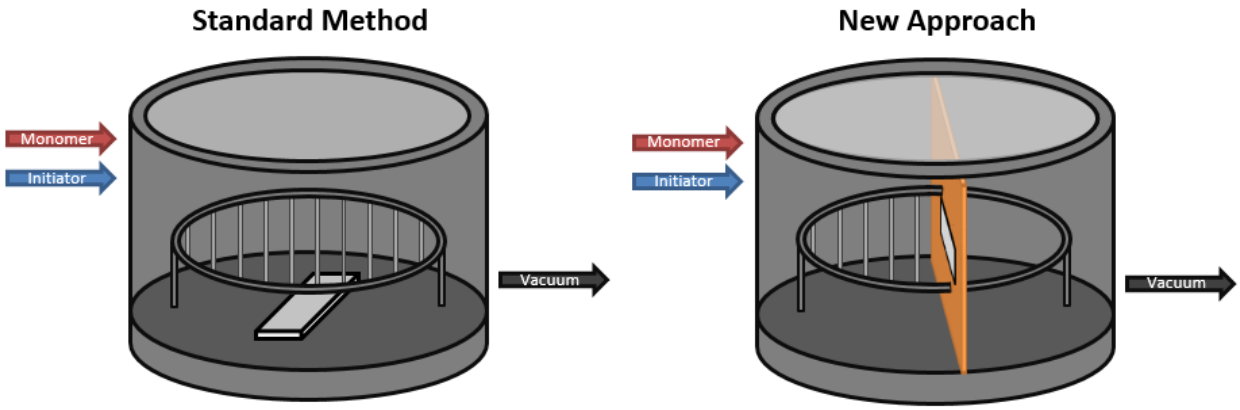

Figure 14: Schematics of the iCVD chamber demonstrating the standard method and the new approach using the scaffold

6.5. Membrane Distillation Protocol

PAN and PVDF nanofiber membranes, and a Millipore PVDF membrane (effective area of 3 x 1 inch^2) were tested in a DCMD set-up. The operating conditions were identical for each membrane. The feed solution was a 5M NaCl solution and DI water was used as the permeate solution. A 30°C temperature difference was maintained between the two streams, where the feed was kept at 50°C and the permeate at 20°C. The permeate flux was measured over the 6-hour duration of the experiment by measuring the change in weight of the permeate tank. Salt rejection was calculated by measuring the conductivity of the permeate tank. Experiments were performed in triplicate for each membrane type.

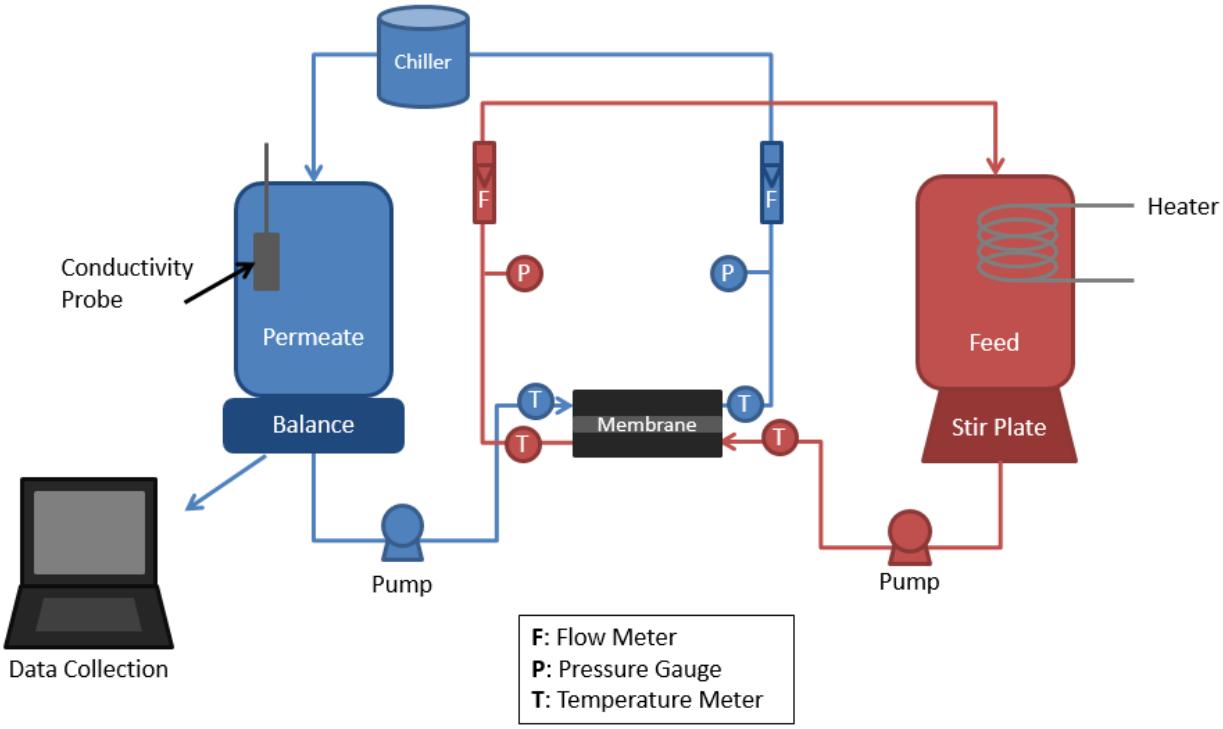

Figure 15: Direct Contact Membrane Distillation Schematic

The performance metrics used to characterize the performance of the membranes in MD are water flux and salt rejection percentage. Water flux (J_w) is the flow rate of water through the

membrane per unit area. This quantity is measured gravimetrically by recording the weight change of the permeate tank over time using a balance and is measured in units of LMH. It is calculated by **Equation 5**:

$$J_w = \frac{\Delta w}{\rho A t} \quad (5)$$

Salt rejection is the percentage of solute rejected by the membrane. The rejection can be calculated by **Equation 6** by considering the difference in concentration between the feed (C_f) and permeate (C_p) tanks:

$$R = \left(1 - \frac{C_p}{C_{f,i}}\right) \times 100 \quad (6)$$

Conductivity measurements were taken from the permeate tank using a conductivity meter. These measurements can be converted from conductivity to concentration using a correlation factor. To find the solute concentration in the permeate tank, **Equation 7** was used, which considers the initial and final concentrations of the permeate tank (C_{pi} and C_{pf}), as well as the initial volume of the permeate tank and total volume change during the experiment (V_{pi} and ΔV).

$$C_p = \frac{C_{p,f}(V_{p,i}+\Delta V) - C_{p,i}V_{p,i}}{\Delta V} \quad (7)$$

These metrics were used to investigate the performance of the membranes coated using the 3D printed scaffold to see if the membranes are suitable for use in MD.

6.6. Contact Angle

Contact Angle measurements were taken using a Cam 101 series contact angle goniometer (KSV Company Linthicum Heights, MD). Membrane samples were taped to a glass slide and the contact angle was measured using DI water. The contact angle was averaged based

on five tests. Both front and back sides of each membrane were tested. Contact angle goniometry can be used to gauge the wettability or hydrophobicity of a surface. Higher contact angles yield higher hydrophobicity and should yield better MD performance.

6.7. Dynamic Mechanical Analysis (DMA)

The stress at breakage was tested using a Dynamic Mechanical Analyzer 2980 from TA Instruments. Tests were run at room temperature and at a ramp rate of 1 N/min. Universal Analysis software from TA Instruments was used to analyze the data. The tensile strength and Young's modulus were obtained from the stress/strain curve generated.

7. Results

Before working with hydrophilic PAN membranes, membrane distillation experiments were first carried out with PVDF membranes to generate a benchmark with which to compare the membranes coated using iCVD. One membrane was a 0.45 μm Millipore non-electrospun commercial membrane. The other membrane was an electrospun PVDF membrane fabricated using the same procedure as the PAN membranes. Both PVDF membranes exhibited 100% salt rejection without any modification, reflecting the inherent hydrophobicity of PVDF. The electrospun membrane exhibited a significantly higher water flux as well.

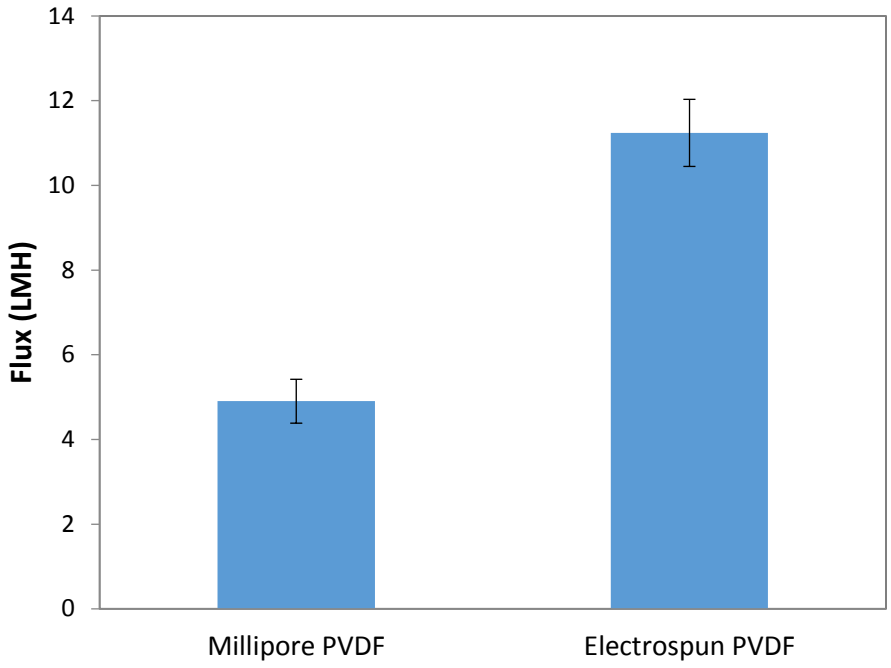

Figure 16: Water flux comparison between commercial Millipore PVDF membrane and electrospun PVDF

Once a benchmark for comparison had been made, electrospun mats were then coated with DVB using iCVD. Previous work in the group found that the standard protocol for coating pDVB on PAN membranes required 100 minutes of deposition on each side of the membrane (200 minutes total) to achieve adequate MD hydrophobicity. Membranes were first coated for 200 minutes using the scaffold followed by 100 and 50 minutes. In these experiments, the deposition was conducted on only one side to elucidate if the new coating method could achieve adequate hydrophobicity on the opposite side of the membrane not directly exposed to the precursors.

Before testing these samples in MD, it was important to see if there were any observable changes to the membrane after iCVD coating. SEM pictures were taken of both the uncoated and

coated electrospun membrane samples to see if there was any noticeable change to the morphology of the membrane.

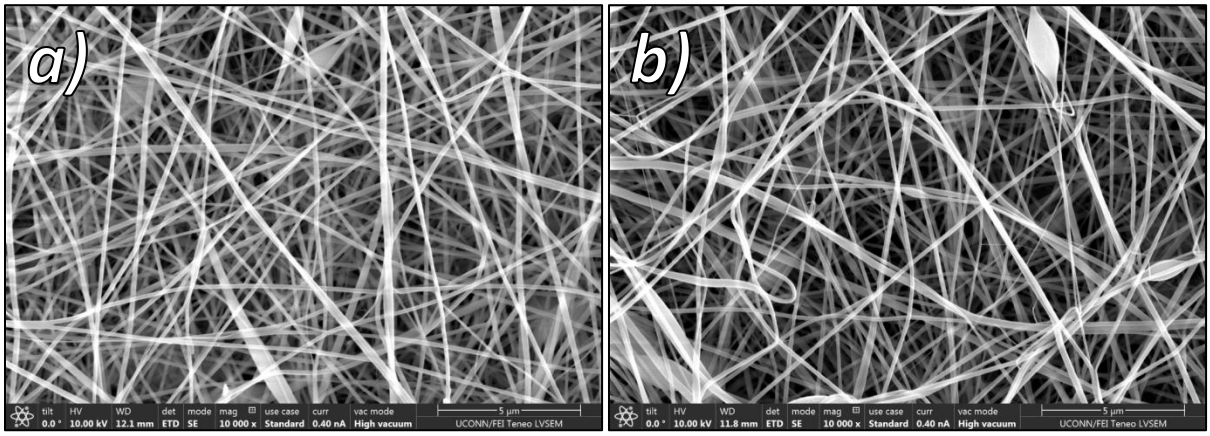

Figure 17: SEM pictures of a) an uncoated electrospun PAN membrane and b) a coated electrospun PAN membrane modified via the scaffold iCVD method

When comparing the coated and uncoated membranes, there was no visible change in nanofiber morphology. While this did not prove that the membrane has been conformally coated, it did imply that the coating process did not cause any damage or change to the membrane that could inhibit its performance. The pores appeared unobstructed, which should allow for water flux to be observed if the membrane did not wet out during the process.

Contact angle measurements were then taken on the membranes, which gave an indication of their hydrophobicity. For the shortest deposition time, measurements were taken of both a membrane coated in the scaffold and a membrane coated in the standard orientation. The membrane coated using the scaffold exhibited superior hydrophobicity on both sides of the membrane: the side directly exposed to the precursors, and the side coated via diffusion through the membrane. The contact angle measurements suggested that the membranes would be viable for MD.

DVB Coated PAN Membranes	Side of Membrane Directly Exposed to Precursors		Side of Membrane Not in Direct Contact with Precursors	
Standard Coating Orientation	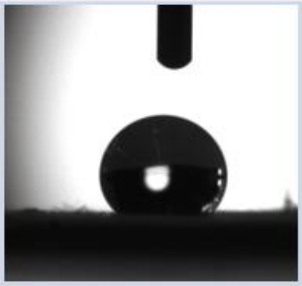	122 ± 4.3	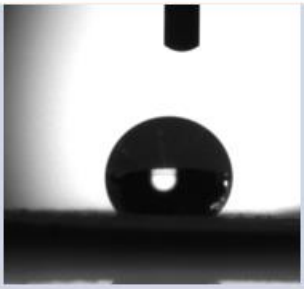	118 ± 4.0
New Coating Orientation with Scaffold	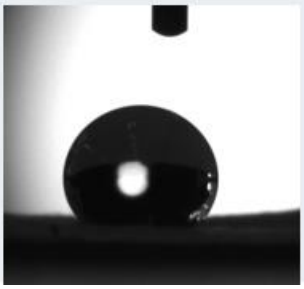	135 ± 4.8	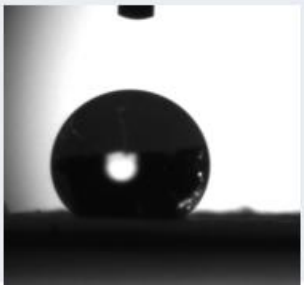	147 ± 4.3

Figure 18: Contact angle measurements of each side of PAN membranes coated with DVB for 50 minutes on one side of the membrane using the standard iCVD method and the scaffold iCVD method

After the positive SEM and contact angle results, the membrane performance was tested. It was observed that the membranes coated for 200, 100, and 50 minutes all exhibited 100% salt rejection in MD and did not wet out during the process. The membranes also exhibited good water flux which increased as coating time decreased. This is a result of smaller fiber diameters creating larger pores during the shorter coating times. The longer coating times allow for more deposition to occur on the fibers increasing their diameter (not observable under SEM), which therefore decreases the pore size. The water flux observed from the 50 minute membrane was comparable to the electrospun PVDF membrane.

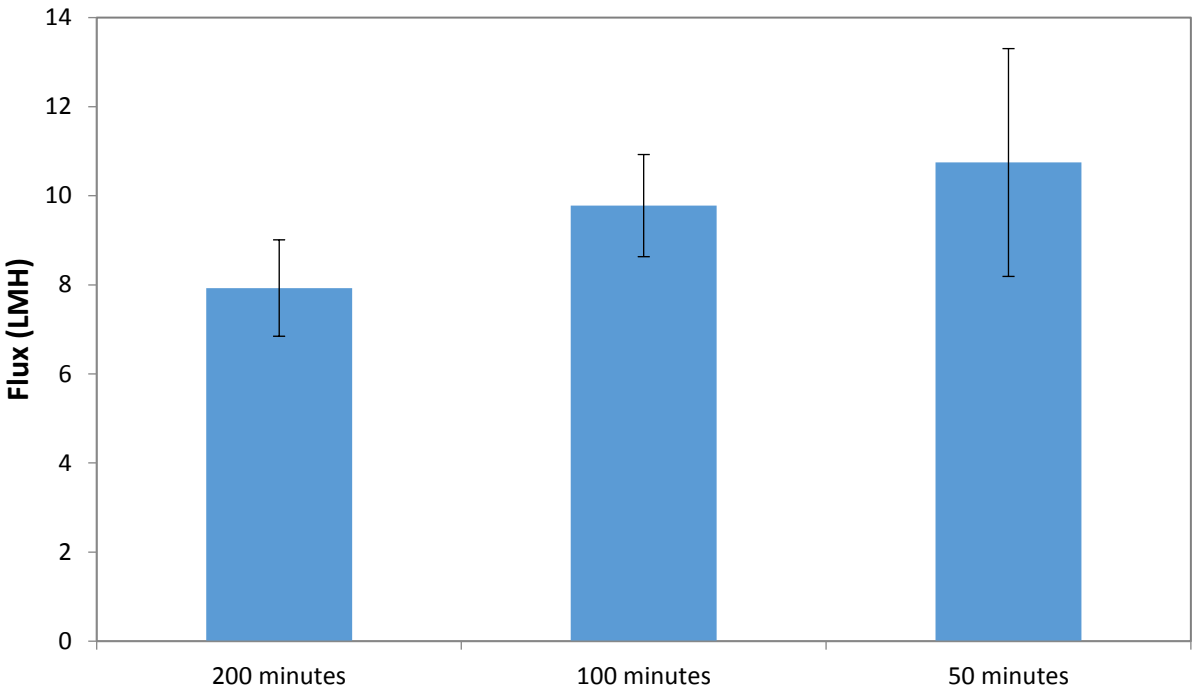

Figure 19: Water flux comparison between iCVD deposition times of pDVB-coated PAN membranes using the 3D printed scaffold

Coating time was then decreased further to 30 minutes. The membrane coated using the scaffold was compared to a membrane coated using the standard method. The membrane coated using the scaffold exhibited 100% salt rejection and good water flux. Surprisingly, when the control membrane affixed to the stage was tested in MD, the membrane also exhibited 100% salt rejection. This finding conflicted with the original hypothesis that membranes coated while affixed to the stage required two sides of coating to be viable for MD.

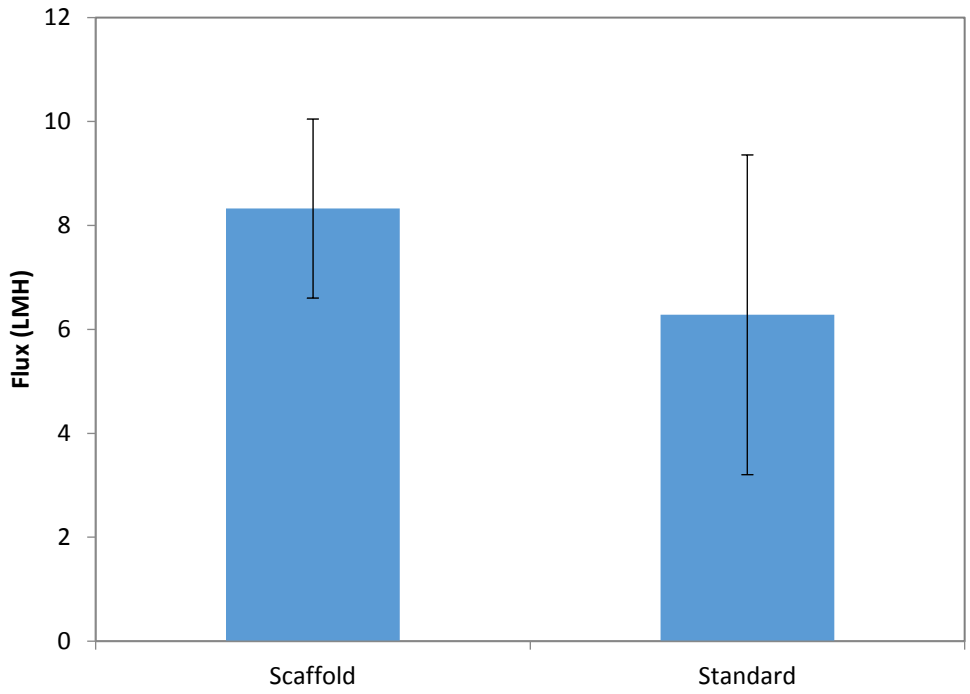

Figure 20: Water flux comparison between PAN membranes coated with DVB for 30 minutes using the standard iCVD method and the scaffold iCVD method

Previous work on iCVD has shown that monomer deposition rate is strongly influenced by substrate temperature and that lower substrate temperatures yield higher deposition rates [34]. In the scaffold orientation, there is no temperature control. In order to eliminate temperature as a variable and focus solely on the effect of convective flow, a mesh allowing convective flow and a mesh inhibiting convective flow were printed and then used to support the membrane in the scaffold. The mesh inhibiting convective flow should prevent convective flow through the membrane similar to how the membrane is coated using the standard method, eliminating the temperature variable in the comparison and offering better insight into the role of convective flow in coating the membrane.

Contact angle measurements were then conducted on a membrane coated with the mesh allowing convective flow and a membrane coated with a mesh inhibiting convective flow. The mesh allowing convective flow resulted in a higher contact angle on both sides of the membrane compared to the mesh inhibiting convective flow.

DVB Coated PAN Membranes	Side of Membrane Directly Exposed to Precursors	Side of Membrane Not in Direct Contact with Precursors
Convective Flow	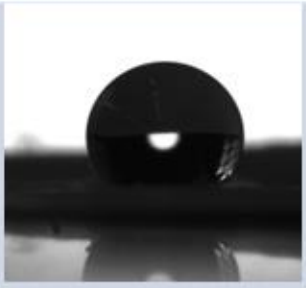 149 ± 3.4	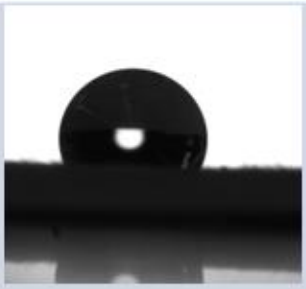 141 ± 1.5
No Convective Flow	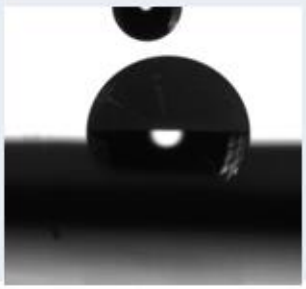 135 ± 0.9	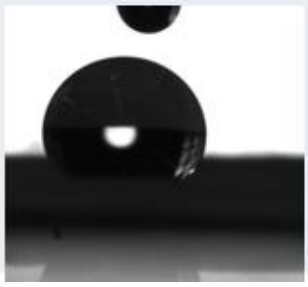 127 ± 0.7

Figure 21: Contact angle measurements comparison after 30 minutes of deposition between membranes coated using a mesh that allows convective flow and a mesh that inhibits convective flow

The membrane coated using the mesh inhibiting convective flow was then subjected to MD experiments. This membrane also both exhibited good flux and 100% salt rejection over the six hour experiment. There was more variability in the mesh inhibiting convective flow results. Both the mesh allowing convective flow and the mesh inhibiting convective flow showed an

average similar performance after 30 minutes of coating. The next step was to further decrease the coating time to see if any deviation between the two membranes could be observed.

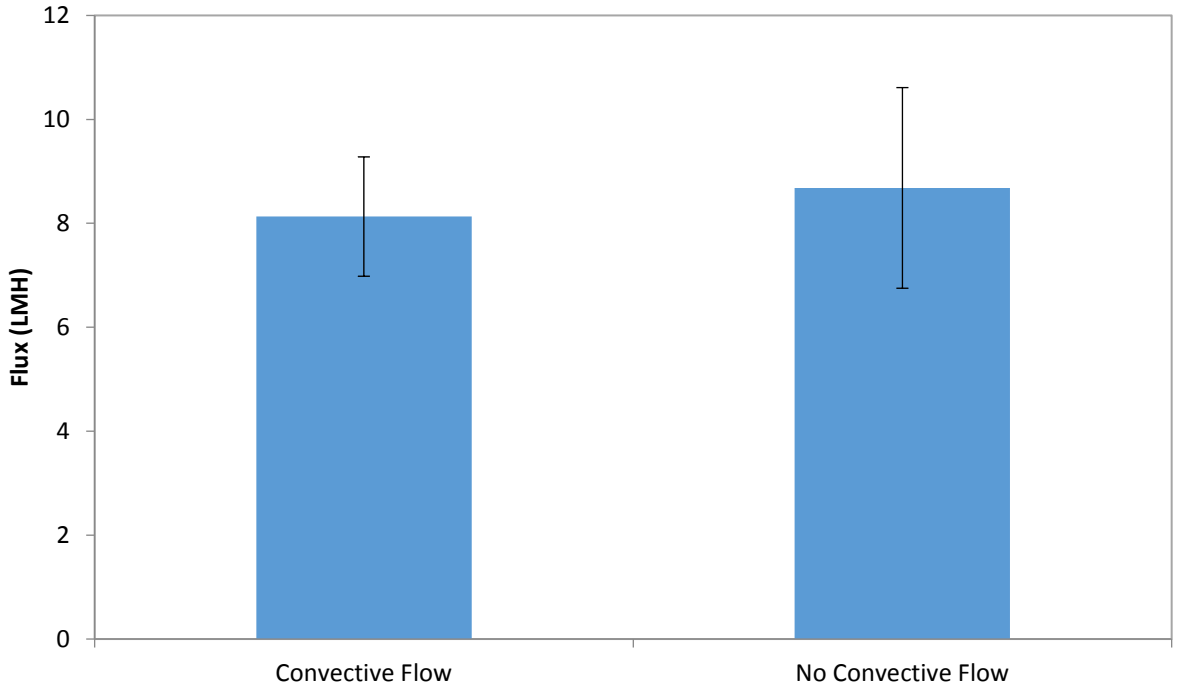

Figure 22: Water flux comparison between membranes coated using a mesh that allows convective flow and a mesh that inhibits convective flow

The coating time was then decreased to 15 minutes. Contact angle measurements were taken on both sides of each membrane. It was found that the membrane supported by the mesh allowing convective flow exhibited a higher contact angle on both sides than the membrane supported by the mesh inhibiting convective flow. The back side of the membrane coated using the mesh inhibiting convective flow completely wetted out during the contact angle experiment, while the membrane coated using the mesh allowing convective flow still exhibited hydrophobicity.

DVB Coated PAN Membranes	Side of Membrane Directly Exposed to Precursors		Side of Membrane Not in Direct Contact with Precursors	
Convective Flow	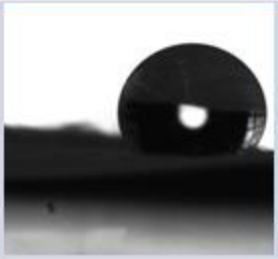	136 ± 0.6	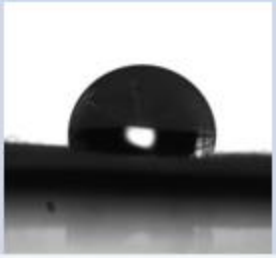	125 ± 0.4
No Convective Flow	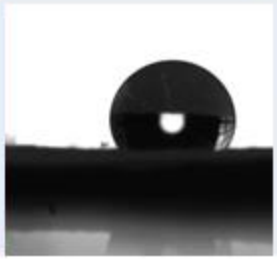	124 ± 0.5		NA

Figure 23: Contact angle measurements of each side of PAN membranes coated with DVB for 15 minutes using the standard iCVD method and the scaffold iCVD method

The membrane coated using the mesh inhibiting convective flow was not viable for MD as the backside was completely hydrophilic. Preliminary data for the membrane coated for 15 minutes using the mesh allowing convective flow showed that the sample did not fail immediately. The membrane did, however, fail before the 6-hour experiment was completed and no longer exhibited 100% salt rejection. When the membrane was coated for 20 minutes using the mesh allowing convective flow, the membrane exhibited good flux and 100% salt rejection over the 6-hour period.

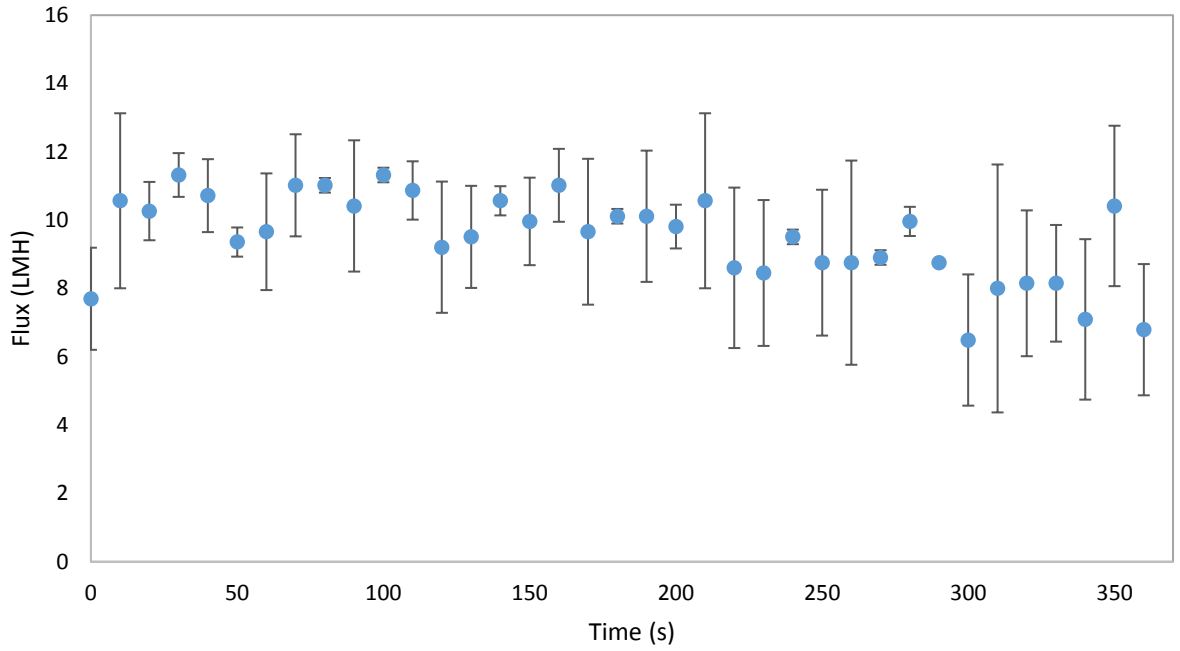

Figure 24: Water flux performance over six hours for a membrane supported by the mesh allowing convective flow and coated for 20 minutes

In addition to hydrophobicity and thermal stability, mechanical stability is another important MD membrane characteristic. Various coated and uncoated membranes were subjected to DMA tests to calculate their Young's modulus and tensile strength. It was observed that the coated membranes yielded a significantly higher tensile strength than the uncoated membranes. The Young's modulus was similar for all membranes.

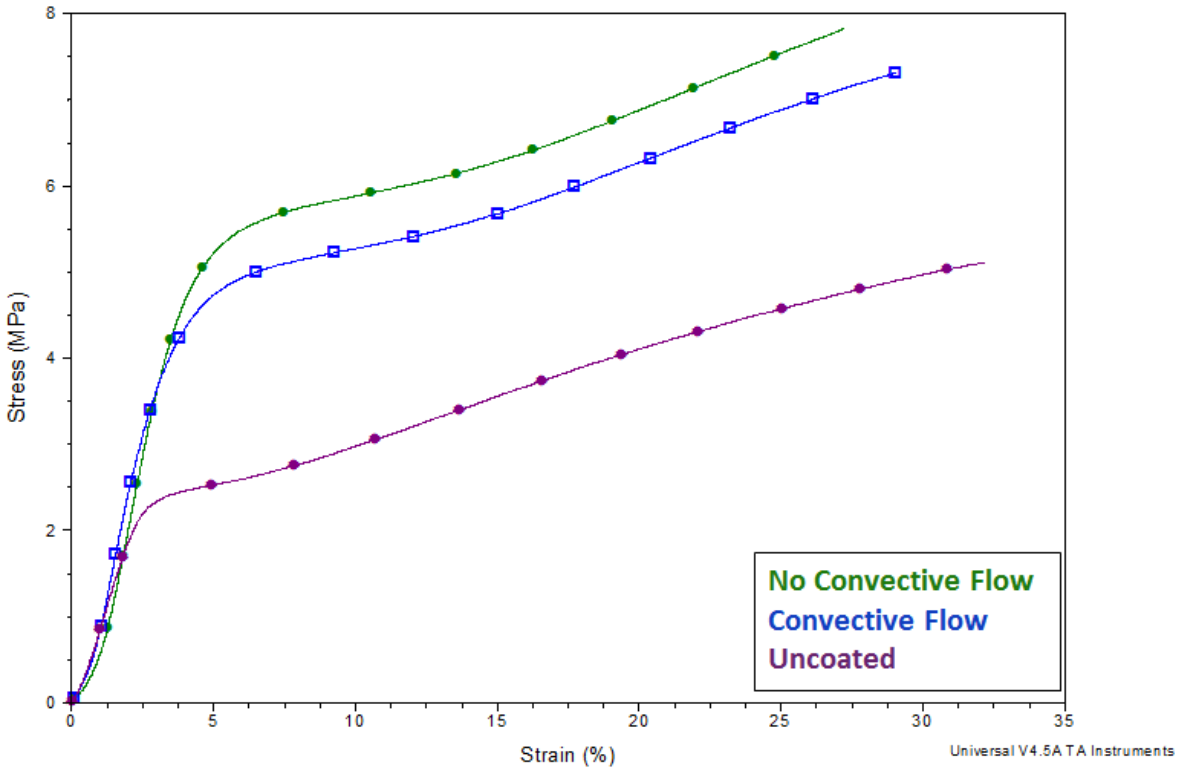

Figure 25: Stress/Strain Curve of uncoated PAN membranes and membranes coated for 15 and 30 minutes using the mesh allowing convective flow, mesh inhibiting convective flow, and standard orientation

8. Discussion

In the conventional method, the membrane was taped flat on the chilled stage floor. The monomer and initiator must diffuse down through the chamber to adsorb onto the fibers. The rate of deposition is controlled via temperature. Adsorption was found to be enhanced at lower substrate temperatures. Higher deposition rates were reported for membranes held at lower stage temperatures. The method relies on temperature as the rate-determining parameter. In order to achieve adequate hydrophobicity, the membrane must be coated twice, once on each side, which adds additional dead time to the process as the chamber must be purged and then brought back

under vacuum again. There is a low conversion rate for the polymerization and the much of the reactants are irreversibly wasted [32].

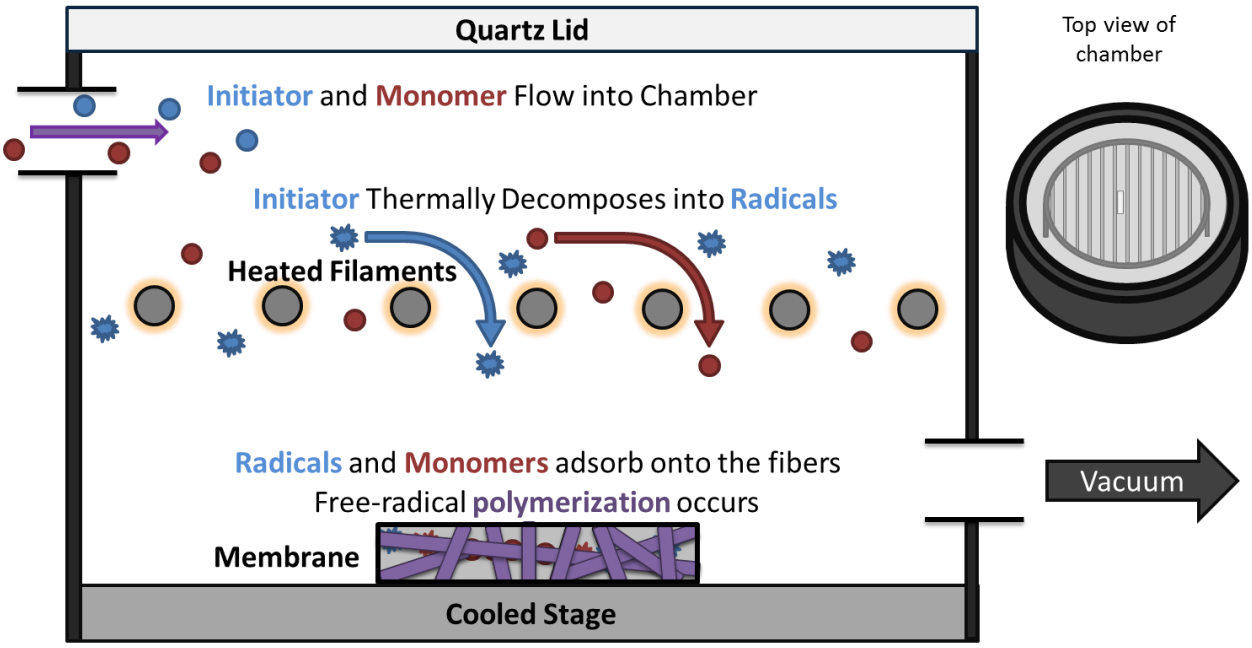

Figure 26: Side view of the iCVD chamber depicting the deposition process in the standard method

In the new approach discussed in this thesis, the membrane is held in place through the use of a scaffold at a position normal to the flow of reactants into the chamber. This position allows for convective flow of reactants through the membrane rather than relying strictly on natural diffusion down through the chamber. In this configuration, the only path for the reactants to exit the chamber is through the membrane. Deposition is not limited by only diffusion down through the chamber as in the standard method. Convective flow through the membrane allows for another mechanism for coating to occur on the membrane fibers that could potentially coat the backside of the membrane eliminating the need for two rounds of coating.

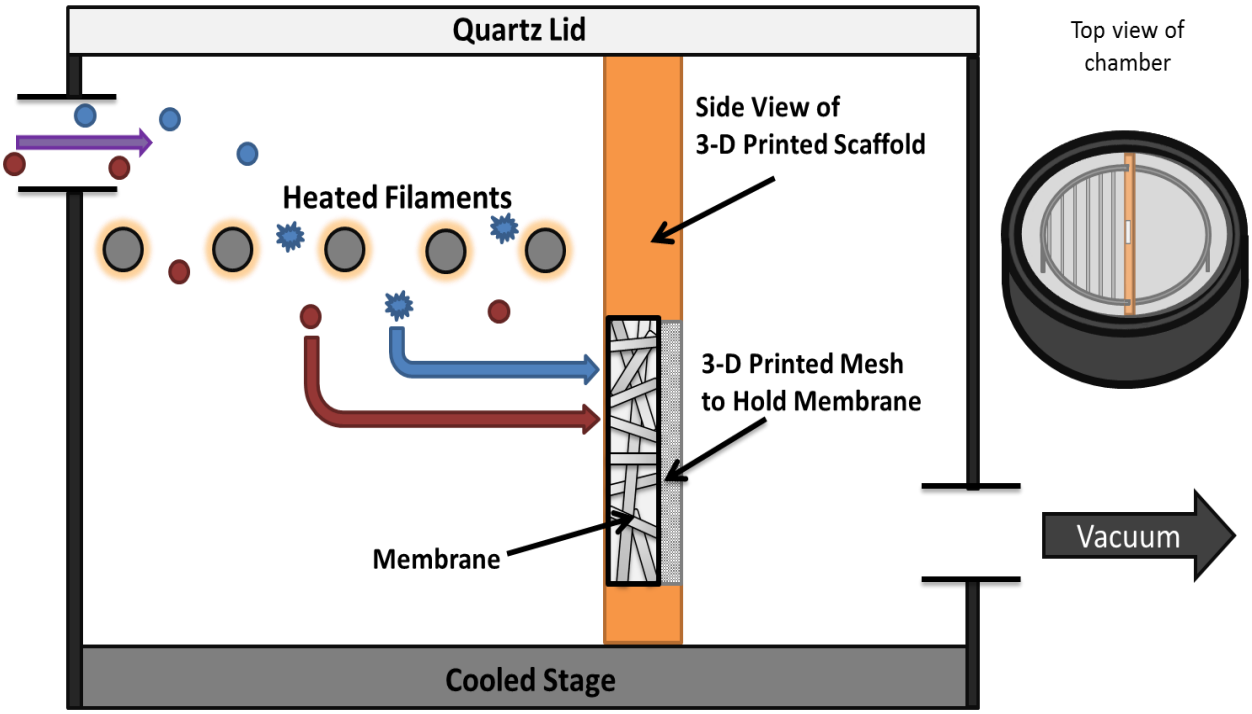

Figure 27: Side view of the iCVD chamber depicting the deposition process with the use of the scaffold

The higher contact angles exhibited by the mesh allowing convective flow imply that convective flow through the membrane allows for better coating of the side not directly exposed to the precursors. This was best indicated by the 15 minute contact angle test shown in **Figure 23** where the back side of the membrane coated using the mesh inhibiting convective flow completely wetted out after the experiment. Convective flow does enhance the coating of the opposite side of the membrane. The improved coating technique eliminates the necessity for two rounds of coating as required in the standard method, removing the dead time when the system needs to be purged in order to open the chamber and switch the side of the membrane directly exposed to the precursors.

The coating time was also significantly reduced using this process. The previous shortest coating time shown in literature was 35 minutes on each side, totaling 70 minutes [50]. Using the new method, the coating time can be reduced to a single 20 minute run. This process is more environmentally friendly as the lower time allows for fewer reactants to be used while still maintaining adequate hydrophobicity.

The water flux observed through the membranes coated using the new approach are comparable with that observed through electrospun PVDF membranes. Not only can hydrophilic membranes be modified for use in MD, they also show promise as competitive commercial membranes due to their high flux and high salt rejection. The ability to modify hydrophilic fibers greatly expands the range of polymers that can be used as MD membranes. Other hydrophilic polymers can be electrospun to test if the water flux can be further improved. The mechanical strength was also shown to increase after this process, which further expands the range of membranes that can be used by improving the robustness of fragile membranes.

Coating time could also be further reduced by introducing a cooling component into the scaffold design. This could be achieved by either adding a cooling device into the actual scaffold or fabricating the device out of metal to allow for heat transfer from the cooled stage to the scaffold. Considering the MD results for membranes coated using the standard method, temperature does play a role in the coating process, and higher deposition rates are observed with lower substrate temperatures. Combining the benefits of convective flow and lower temperatures could yield an even faster coating time, further improving the efficiency and environmental impact of this process.

9. Conclusion

The 3D printed scaffold offers a superior way for coating nanofiber membranes using iCVD. This method does not require coating both sides of the membrane, reducing the process dead time. It was found that convective flow enhances the coating of the side of the membrane not in direct contact with the precursors. This was elucidated through the contact angle comparison between iCVD coated membranes supported in the scaffold by the mesh which allowed convective flow and the mesh which inhibited it. The membrane supported by the mesh allowing convective flow retained hydrophobicity after 15 minutes of coating while the other did not.

The process has also been shown to yield viable MD membranes coated with pDVB faster than any reported in literature. This results in a reduction in the environmental impact by requiring fewer precursors to be used to achieve adequate hydrophobicity. The reduction in coating time and process dead time is more favorable for commercial applications as well. The mechanical strength of the electrospun membranes were also enhanced after the iCVD coating process. The method demonstrates an improved way of iCVD coating nanofiber materials that can be applied to other membrane coating applications and for other polymers. It can be further expanded to other nanofiber or porous materials that require complete coating on both sides of the substrate.

10. References

[1] United Nations, 64/292. The human right to water and sanitation, Gen. Assem. 64 (2010) 3. http://www.un.org/es/comun/docs/?symbol=A/RES/64/292&lang=E.

[2] Water | United Nations, (n.d.). http://www.un.org/en/sections/issues-depth/water/ (accessed July 21, 2017).

[3] D.M. Cutler, G. Miller, The role of public health improvements in health advances: the 20th century United States, Natl. Bur. Econ. Res. Work. Pap. No. 10511. (2004). http://www.nber.org/papers/w10511.pdf (accessed July 21, 2017).

[4] L. Liu, H.L. Johnson, S. Cousens, J. Perin, S. Scott, J.E. Lawn, I. Rudan, H. Campbell, R. Cibulskis, M. Li, C. Mathers, R.E. Black, Global, regional, and national causes of child mortality: an updated systematic analysis for 2010 with time trends since 2000, Lancet. 379 (2012) 2151–2161. doi:10.1016/S0140-6736(12)60560-1.

[5] Global Water Shortage: Water Scarcity & How to Help - Page 2, (n.d.). https://thewaterproject.org/water-scarcity/water_scarcity_2 (accessed May 8, 2017).

[6] Drought and Climate Change | Center for Climate and Energy Solutions, (n.d.). https://www.c2es.org/science-impacts/extreme-weather/drought (accessed April 25, 2017).

[7] Where is Earth's water? USGS Water-Science School, (n.d.). https://water.usgs.gov/edu/earthwherewater.html (accessed April 25, 2017).

[8] California's Worst Drought in History: The Breakdown, (n.d.). http://www.visualnews.com/2015/04/13/californias-worst-drought-in-history-the-breakdown/ (accessed May 8, 2017).

[9] M. Sadrzadeh, T. Mohammadi, Sea water desalination using electrodialysis, Desalination. 221 (2008) 440–447. doi:10.1016/j.desal.2007.01.103.

[10] B. Van der Bruggen, C. Vandecasteele, Distillation vs. membrane filtration: overview of process evolutions in seawater desalination, Desalination. 143 (2002) 207–218. doi:10.1016/S0011-9164(02)00259-X.

[11] L.M. Camacho, L. Dumée, J. Zhang, J. de Li, M. Duke, J. Gomez, S. Gray, Advances in membrane distillation for water desalination and purification applications, Water (Switzerland). 5 (2013) 94–196. doi:10.3390/w5010094.

[12] S. Al-Obaidani, E. Curcio, F. Macedonio, G. Di Profio, H. Al-Hinai, E. Drioli, Potential of membrane distillation in seawater desalination: Thermal efficiency, sensitivity study and cost estimation, J. Memb. Sci. 323 (2008) 85–98. doi:10.1016/j.memsci.2008.06.006.

[13] L. Martínez-Díez, M.I. Vázquez-Gonzàlez, Temperature polarization in mass transport through hydrophobic porous membranes, AIChE J. 42 (1996) 1844–1852. doi:10.1002/aic.690420706.

[14] K.W. Lawson, D.R. Lloyd, Membrane distillation, J. Memb. Sci. 124 (1997) 1–25. https://ac.els-cdn.com/S0376738896002360/1-s2.0-S0376738896002360-main.pdf?_tid=f4d86740-deb3-11e7-b14f-00000aab0f02&acdnat=1513025195_0fba2d8000bcca4bc9198c9dffe59005 (accessed December 11, 2017).

[15] A. Alkhudhiri, N. Darwish, N. Hilal, Membrane distillation: A comprehensive review, Desalination. 287 (2012) 2–18. doi:10.1016/J.DESAL.2011.08.027.

[16] R.B. Saffarini, E.K. Summers, H.A. Arafat, J.H. Lienhard, Technical evaluation of stand-alone solar powered membrane distillation systems, (2012).

doi:10.1016/j.desal.2011.11.044.
[17] H.J. Hwang, K. He, S. Gray, J. Zhang, I.S. Moon, Direct contact membrane distillation (DCMD): Experimental study on the commercial PTFE membrane and modeling, J. Memb. Sci. 371 (2011) 90–98. doi:10.1016/j.memsci.2011.01.020.
[18] L.-T. Huang, P.-S. Hsu, C.-Y. Kuo, S.-C. Chen, J.-Y. Lai, Pore size control of PTFE membranes by stretch operation with asymmetric heating system, DES. 233 (2008) 64–72. doi:10.1016/j.desal.2007.09.028.
[19] P. Wang, T.-S. Chung, Recent advances in membrane distillation processes: Membrane development, configuration design and application exploring, J. Memb. Sci. 474 (2015) 39–56. doi:10.1016/j.memsci.2014.09.016.
[20] E. Drioli, A. Ali, F. Macedonio, Membrane distillation: Recent developments and perspectives, DES. 356 (2014) 56–84. doi:10.1016/j.desal.2014.10.028.
[21] Z.-M. Huang, Y.-Z. Zhang, M. Kotaki, S. Ramakrishna, A review on polymer nanofibers by electrospinning and their applications in nanocomposites, Compos. Sci. Technol. 63 (2003) 2223–2253. doi:10.1016/S0266-3538(03)00178-7.
[22] Z.-Q. Dong, X. Ma, Z.-L. Xu, W.-T. You, F. Li, Superhydrophobic PVDF–PTFE electrospun nanofibrous membranes for desalination by vacuum membrane distillation, Desalination. 347 (2014) 175–183. doi:10.1016/j.desal.2014.05.015.
[23] Y. Liao, R. Wang, M. Tian, C. Qiu, A.G. Fane, Fabrication of polyvinylidene fluoride (PVDF) nanofiber membranes by electro-spinning for direct contact membrane distillation, J. Memb. Sci. 425 (2013) 30–39. doi:10.1016/j.memsci.2012.09.023.
[24] L. Francis, H. Maab, A. AlSaadi, S. Nunes, N. Ghaffour, G.L. Amy, Fabrication of electrospun nanofibrous membranes for membrane distillation application, Desalin. Water Treat. 51 (2013) 1337–1343. doi:10.1080/19443994.2012.700037.
[25] M. Essalhi, M. Khayet, Self-sustained webs of polyvinylidene fluoride electrospun nanofibers at different electrospinning times: 1. Desalination by direct contact membrane distillation, J. Memb. Sci. 433 (2013) 167–179. doi:10.1016/j.memsci.2013.01.023.
[26] C.-I. Su, J.-H. Shih, M.-S. Huang, C.-M. Wang, W.-C. Shih, Y.-S. Liu, A Study of Hydrophobic Electrospun Membrane Applied in Seawater Desalination by Membrane Distillation, Fibers Polym. 13 (2012) 698–702. doi:10.1007/s12221-012-0698-3.
[27] M. Khayet, T. Matsuurab, Application of surface modifying macromolecules for the preparation of membranes for membrane distillation, Desalin. ELSEVIER Desalin. 158 (2003) 1–56. www.elsevier.cotn/locate/desal (accessed November 6, 2017).
[28] A. Razmjou, E. Arifin, G. Dong, J. Mansouri, V. Chen, Superhydrophobic modification of TiO 2 nanocomposite PVDF membranes for applications in membrane distillation, (2012). doi:10.1016/j.memsci.2012.06.004.
[29] Z. Jin, D.L. Yang, S.H. Zhang, X.G. Jian, Hydrophobic modification of poly(phthalazinone ether sulfone ketone) hollow fiber membrane for vacuum membrane distillation, J. Memb. Sci. 310 (2008) 20–27. doi:10.1016/j.memsci.2007.10.021.
[30] S.H. Baxamusa, S.G. Im, K.K. Gleason, G. Barbasthasis, S. Borros, K.K. Gleason, M.F. Rubner, G.C. Rutledge, C.R. Towns, J.H. Burroughes, R.H. Friend, Initiated and oxidative chemical vapor deposition: a scalable method for conformal and functional polymer films on real substrates, Phys. Chem. Chem. Phys. 11 (2009) 5227. doi:10.1039/b900455f.
[31] K.K. Gleason, ed., CVD Polymers: Fabrication of Organic Surfaces and Devices, First, Wiley-VCH Verlag GmbH & Co. KGaA., 2015.
[32] J.-H. Park, T.S. Sudarshan, Chemical Vapor Deposition, ASM International, 2001.

https://www.scribd.com/doc/75746558/Chemical-Vapor-Deposition-Surface-Engineering-Series-V-2-ASMI (accessed April 26, 2017).
[33] S.G. Im, K.K. Gleason, Solvent-free modification of surfaces with polymers: The case for initiated and oxidative chemical vapor deposition (CVD), AIChE J. 57 (2011) 276–285. doi:10.1002/aic.12522.
[34] K.K.S. Lau, K.K. Gleason, Initiated chemical vapor deposition (iCVD) of poly(alkyl acrylates): An experimental study, Macromolecules. 39 (2006) 3688–3694. doi:Doi 10.1021/Ma0601619.
[35] K.K.S. Lau, K.K. Gleason, Initiated Chemical Vapor Deposition (iCVD) of poly(alkyl acrylates): A kinetic model, Macromolecules. 39 (2006) 3695–3703. doi:10.1021/ma0601621.
[36] A. Suresh, D. Anastasio, D.D. Burkey, Potential of hexyl acrylate monomer as an initiator in photo-initiated CVD, Chem. Vap. Depos. 20 (2014) 5–7. doi:10.1002/cvde.201304322.
[37] K. Chan, K.K. Gleason, Photoinitiated Chemical Vapor Deposition of Polymeric Thin Films Using a Volatile Photoinitiator, Langmuir. 21 (2005) 11773–11779. doi:10.1021/la051469g.
[38] T.P. Martin, S.E. Kooi, S.H. Chang, K.L. Sedransk, K.K. Gleason, Initiated chemical vapor deposition of antimicrobial polymer coatings, Biomaterials. 28 (2007) 909–915. doi:10.1016/j.biomaterials.2006.10.009.
[39] R. Yang, K.K. Gleason, Ultrathin antifouling coatings with stable surface zwitterionic functionality by initiated chemical vapor deposition (iCVD), Langmuir. 28 (2012) 12266–12274. doi:10.1021/la302059s.
[40] F. Guo, A. Servi, A. Liu, K.K. Gleason, G.C. Rutledge, Desalination by membrane distillation using electrospun polyamide fiber membranes with surface fluorination by chemical vapor deposition, ACS Appl. Mater. Interfaces. (2015) 8225–8232. doi:10.1021/acsami.5b01197.
[41] GVD Corporation | Dedicated to improving the surface of things, (n.d.). http://www.gvdcorp.com/ (accessed April 26, 2017).
[42] S. Calechman, Commercializing a new generation of polymer coatings | MIT News, (2015). http://news.mit.edu/2015/gvd-commercializing-new-generation-polymer-coatings-0112 (accessed April 26, 2017).
[43] L.D. Tijing, J.S. Choi, S. Lee, S.H. Kim, H.K. Shon, Recent progress of membrane distillation using electrospun nanofibrous membrane, J. Memb. Sci. 453 (2014) 435–462. doi:10.1016/j.memsci.2013.11.022.
[44] A. Matin, G. Ozaydin-ince, Z. Khan, S. Mohammad, J. Zaidi, K. Gleason, D. Eggenspiler, Random copolymer films as potential antifouling coatings for reverse osmosis membranes, Desalin. Water Treat. 34 (2011) 100–105. doi:10/5004/dwt.2011.2804.
[45] A. Matin, Z. Khan, K.K. Gleason, M. Khaled, S.M.J. Zaidi, A. Khalil, P. Moni, R. Yang, Surface-modified reverse osmosis membranes applying a copolymer film to reduce adhesion of bacteria as a strategy for biofouling control, Sep. Purif. Technol. 124 (2014) 117–123. doi:10.1016/j.seppur.2013.12.032.
[46] G. Ozaydin-Ince, A. Matin, Z. Khan, S.M.J. Zaidi, K.K. Gleason, Surface modification of reverse osmosis desalination membranes by thin-film coatings deposited by initiated chemical vapor deposition, Thin Solid Films. 539 (2013) 181–187. doi:10.1016/j.tsf.2013.04.133.
[47] R. Yang, J. Xu, G. Ozaydin-Ince, S.Y. Wong, K.K. Gleason, Surface-tethered zwitterionic

ultrathin antifouling coatings on reverse osmosis membranes by initiated chemical vapor deposition, Chem. Mater. 23 (2011) 1263–1272. doi:10.1021/cm1031392.
[48] A. Asatekin, K.K. Gleason, Polymeric nanopore membranes for hydrophobicity-based separations by conformal initiated chemical vapor deposition, Nano Lett. 11 (2011) 677–686. doi:10.1021/nl103799d.
[49] M. Gupta, K.K. Gleason, Surface modification of high aspect ratio structures with fluoropolymer coatings using chemical vapor deposition, Thin Solid Films. 517 (2009) 3547–3550. doi:10.1016/j.tsf.2009.01.037.
[50] A.T. Servi, J. Kharraz, D. Klee, K. Notarangelo, B. Eyob, E. Guillen-Burrieza, A. Liu, H.A. Arafat, K.K. Gleason, A systematic study of the impact of hydrophobicity on the wetting of MD membranes, J. Memb. Sci. 520 (2016) 850–859. doi:10.1016/j.memsci.2016.08.021.
[51] J. Wang, A. Goyanes, S. Gaisford, A.W. Basit, Stereolithographic (SLA) 3D printing of oral modified-release dosage forms, Int. J. Pharm. 503 (2016) 207–212. doi:10.1016/j.ijpharm.2016.03.016.